

# Accepted Manuscript

Synthesis and Bioevaluation of Novel Benzodipyrone Derivatives as P-Glycoprotein Inhibitors for Multidrug Resistance Reversal Agents

Chien-Yu Chen, Nai-Yu Liu, Hui-Chang Lin, Chih-Yu Lee, Chin-Chuan Hung, Chih-Shiang Chang



PII: S0223-5234(16)30252-5

DOI: [10.1016/j.ejmech.2016.03.070](https://doi.org/10.1016/j.ejmech.2016.03.070)

Reference: EJMECH 8495

To appear in: *European Journal of Medicinal Chemistry*

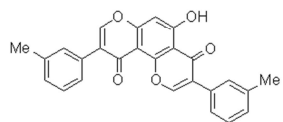
Received Date: 25 December 2015

Revised Date: 9 March 2016

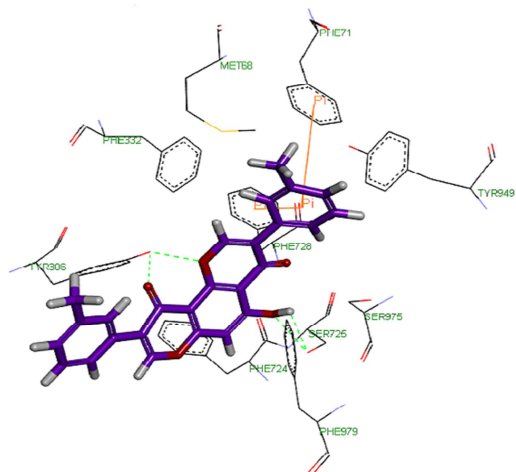
Accepted Date: 25 March 2016

Please cite this article as: C.-Y. Chen, N.-Y. Liu, H.-C. Lin, C.-Y. Lee, C.-C. Hung, C.-S. Chang, Synthesis and Bioevaluation of Novel Benzodipyrone Derivatives as P-Glycoprotein Inhibitors for Multidrug Resistance Reversal Agents, *European Journal of Medicinal Chemistry* (2016), doi: 10.1016/j.ejmech.2016.03.070.

This is a PDF file of an unedited manuscript that has been accepted for publication. As a service to our customers we are providing this early version of the manuscript. The manuscript will undergo copyediting, typesetting, and review of the resulting proof before it is published in its final form. Please note that during the production process errors may be discovered which could affect the content, and all legal disclaimers that apply to the journal pertain.



	<b>5a</b>			
	<i>ABCBI/Flp-In<sup>TM</sup>-293</i>		KBvin	
	IC <sub>50</sub> (nM)	RF	IC <sub>50</sub> (nM)	RF
<b>Paclitaxel</b>	644.78 ± 2.60	1.0	1196.09 ± 44.80	1.0
<b>+5a (10 μM)</b>	40.12 ± 1.37*	16.1	51.67 ± 0.26*	23.1
<b>Vincristine</b>	823.13 ± 15.79	1.0	2867.34 ± 142.36	1.0
<b>+5a (10 μM)</b>	39.11 ± 1.07*	21.0	96.49 ± 1.90*	29.7



ACCEPTED MANUSCRIPT

**Synthesis and Bioevaluation of Novel Benzodipyrone Derivatives as****P-Glycoprotein Inhibitors for Multidrug Resistance Reversal Agents**

Chien-Yu Chen<sup>a</sup>, Nai-Yu Liu<sup>a</sup>, Hui-Chang Lin<sup>a</sup>, Chih-Yu Lee<sup>a</sup>, Chin-Chuan Hung<sup>a,\*</sup>,  
Chih-Shiang Chang<sup>a,\*</sup>

<sup>a</sup>School of Pharmacy, College of Pharmacy, China Medical University, 91,  
Hsueh-Shih Road, Taichung 404, Taiwan, Republic of China.

To whom correspondence should be addressed.

Corresponding Authors

\*For C.S.Chang.: phone, +886-4-22053366#5615; fax, +886-4-22078083;

E-mail: chihshiang@mail.cmu.edu.tw.

\*For C.C.Hung.: phone, +886-4-22053366#5155; fax, +886-4-22078083;

E-mail: cc0206hung@gmail.com.

**ABSTRACT**

Multidrug resistance (MDR) is a phenomenon in which cells become resistant to structurally and mechanistically unrelated drugs, and it is one of the emerging problems in cancer therapy today. The relation between overexpression of the ABC transporter subfamily B member 1 (ABCB1/P-glycoprotein) and resistant cancers has been well characterized. In the present study, we successfully synthesized 52 novel benzodipyranone analogs and evaluated for their P-gp inhibitory activity in a P-gp transfected cell line, *ABCB1/Flp-In*<sup>TM</sup>-293. Among these derivatives, **5a** bearing on the 3-methylphenyl substituent, displayed the most potent P-gp inhibitory activity, which can enable the increase of the intracellular accumulation of P-gp substrate Calcein-AM. **5a** exhibited more potency on promoted anticancer drugs cytotoxicity by reversing P-gp-mediated drug resistance in both *ABCB1/Flp-In*<sup>TM</sup>-293 and KBvin cell lines. In particular, the compound **5a** sensitized *ABCB1/Flp-In*<sup>TM</sup>-293 cells toward paclitaxel, vincristine, and doxorubicin by 16.1, 21.0, and 1.6-fold at 10  $\mu$ M, respectively. Further, **5a** dramatically sensitized the resistant cell line KBvin toward paclitaxel and vincristine by 23.1 and 29.7-fold at 10  $\mu$ M, respectively. It's possible that its mechanism of MDR inhibition can restore the intracellular accumulation of drugs and eventually chemosensitize cancer cells to anticancer drugs and reduce *ABCB1* mRNA expression level.

**Keywords:** multidrug resistance, P-glycoprotein, benzodipyranone, reversal agent.

## 1. Introduction

One of the critical obstacles related to cancer chemotherapy is resistance against anticancer drugs. Therefore, drug resistance is one of the major causes of death in cancer patients. Multidrug resistance (MDR) is a phenomenon in which cancer cells become resistant to structurally and mechanistically unrelated drugs [1-3]. The most widely studied mechanisms with known clinical significance are (a) pumping drugs out of cells via the activation of efflux pumps, such as ATP-dependent transporters [4]; (b) resistance being mediated by reduced drug uptake, such as through cellular endocytosis [5]; (c) activation of detoxifying proteins, such as phase I, II, and III metabolic enzymes [6]; (d) cells activating mechanisms that repair drug-induced DNA, RNA, or protein damage; and (e) disruptions in apoptotic signalling pathways (especially p53 and Bcl-2) allowing cells to become resistant to drug-induced cell apoptosis [7]. Among these mechanisms that have been reported to result in MDR, the most widely studied mechanism is related to the overexpression of P-glycoprotein (P-gp, also known as MDR1 or ABCB1), belonging to the ATP-binding cassette (ABC) family of transport proteins which use the hydrolysis of ATP as the energy source for extruding chemotherapeutic drugs out of cells [8], resulting in lowered intracellular anticancer drug concentrations and leading to drug resistance [9]. Identifying the many agents that can modulate the P-gp transporter that interfere with P-gp by the competitive or noncompetitive inhibition of drug efflux has recently been studied. On the basis of their affinity, specificity, and toxicity, P-gp inhibitors are classified into three generations. First-generation agents such as verapamil [10], cyclosporin A [11], reserpine, quinidine [12], tamoxifen, and trifluoperazine (**Figure 1**), attempt to block P-gp and have been highly successful in doing just that. But these agents often produce disheartening results *in vivo* because their low binding affinities necessitate the use of high doses, resulting in unacceptable toxicity. Second-generation P-gp inhibitors include cyclosporine A analogue valsopodar [13], pipercolinate derivative biricodar and verapamil analogue dexverapamil [14], and these agents have a higher specificity than the first generation inhibitors and are also less toxic. However, they are confounded by unforeseeable pharmacokinetic interactions and interactions with other ABC transporter proteins [15]. Finally, third-generation agents such as anthranilamide tariquidar [16], acridonecarboxamide elacridar [17, 18], and cyclopropylidibenzosuberane zosuquidar that specifically and potently inhibit P-gp function have been developed by using quantitative structure-activity relationships (QSAR) and combinatorial chemistry to conquer the

restrictions of the second generation P-gp inhibitors (**Figure 2**). One of the most hopeful third-generation P-gp inhibitors is tariquidar, but its use was discontinued due to unfavorable toxicity reports in phase III clinical trials [19]. Unfortunately, among these inhibitors, none of them have been approved for clinical use [20].

Among the heterocyclic compounds, benzodipyranone scaffold have rarely been used for research with current information. This class of compounds is available from both chemical synthesis or from natural products [21]. However, only a few studies have explored their bioactivity, such as their antiallergic activity [22]. It is with that in mind that, we developed an interest in benzodipyranone derivatives against P-gp-mediated MDR. In this study, we synthesized a series of new benzodipyranone derivatives as P-gp inhibitors. These novel benzodipyranone analogues were evaluated for their ability to influence the expression of *ABCB1* mRNA, P-gp function inhibitory potency and MDR-reversing activity in P-gp overexpressing cell lines.

**Figure 1** herein

**Figure 2** herein

## 2. Results and discussion

### 2.1. Chemistry

The preparation of benzodipyranone derivatives was illustrated in **Scheme 1**. The synthesis of **3** started from the commercial of phloroglucinol (**1**) and appropriate acetonitrile (**2**) in borontrifluoride etherate ( $\text{BF}_3 \cdot \text{Et}_2\text{O}$ ) was purged of HCl gas and stirred at room temperature for 12-24 h to obtain imine intermediate, which was then hydrolyzed to the corresponding **3**. Subsequently, the preparation of **4a-31a** and **4b-31b** started from the synthesis of a benzodipyranone nucleus by a Vilsmeier–Haack reaction that involved **3**, methanesulfonyl chloride (MsCl), and *N,N*-dimethylformamide (DMF) in borontrifluoride etherate stirred at 120 °C for 2-4 h to eventually afford asymmetrical benzodipyranone-4,10-dione **4a-31a**, and symmetrical benzodipyranone-4,6-dione **4b-31b** of benzodipyranone derivatives.

**Scheme 1** herein

### 2.2. Biological activity

In order to establish the ability of the benzodipyranone derivatives to inhibit the activity of P-gp, all the synthesized analogues were evaluated *in vitro* against MDR

cell lines using the following assays: (a) Calcein-AM assay; (b) MDR reversal activity; and (c) *ABCB1* mRNA expression assay.

### 2.2.1. Enhancement of Calcein-AM uptake into *ABCB1/Flp-In<sup>TM</sup>-293* cells

The effect of the analogues on the activities of P-gp was determined by evaluating Calcein accumulation in *Flp-In<sup>TM</sup>-293* cells that were transfected overexpressing the P-gp transporters. The Calcein-AM assay utilized for the evaluation involved measuring the fluorescent intensity imparted by Calcein, which accumulated in the cells due to the inhibition of P-gp efflux by the benzodipyrone derivatives. In **Table 1** and **Table 2**, the P-gp inhibition fold is reported for each of the tested compounds, with verapamil being used as a reference compound for the P-gp inhibition test. In asymmetrical benzodipyrano-4,10-dione **4a-31a**, the activity results show that the introduction of an electron donating group, compound **4a**, **5a**, **6a**, **7a**, **9a**, and **11a** inhibited P-gp function from 1.53 to 2.05 fold at 5  $\mu$ M (**Table 1**). However, no improved P-gp inhibitory activity was observed among the 3-methoxyphenyl (**8a**), 3-hydroxyphenyl (**10a**), 3,4,5-trimethoxyphenyl (**12a**), and 3,4-methylenedioxyphenyl (**13a**) substitution. Furthermore, compound **14a-27a** were introduced as a series of electron withdrawing substituents, respectively, all resulting in a decreased inhibition of P-gp activity. Further, compound **28a-31a** substituted with thiopen-2-yl (**28a**), 1-naphthyl (**29a**), phenyl (**30a**), and cyclopropyl (**31a**), respectively, were lost against P-gp activity. These results suggest that the substitution of electron donating groups plays an important factor in determining P-gp inhibitory activity.

**Table 1** herein

In addition, the symmetrical benzodipyrano-4,6-dione **4b-31b** were investigated for their P-gp inhibitory activity (**Table 2**). However, all symmetrical benzodipyrone derivatives were inactive toward P-gp modulating effect. These results illustrate that the benzodipyrano-4,10-dione **4a-31a** possibly have a higher degree of reaching a conformation that is more suitable for matching the P-gp substrate binding sites than the corresponding benzodipyrano-4,6-dione **4b-31b**.

**Table 2** herein

### 2.2.2. Chemo-sensitizing effect of target compounds

The assessment of the ability of a given compound tested in our study to enhance the growth inhibitory effects of the anticancer drugs paclitaxel, vincristine, and doxorubicin in resistant cell lines displaying MDR due to P-gp overexpression proved

useful in the quantification and characterization of MDR reversal by inhibition of the MDR phenotype. The reversal effects of selected compounds **5a**, **9a**, and **11a** on the MDR phenotype were investigated on the P-gp-transfected cell line *ABCB1*/Flp-In<sup>TM</sup>-293 and its parent Flp-In<sup>TM</sup>-293. The MDR reversal effect of benzodipyrone derivatives was compared by measuring the reversal fold (RF), defined as the ratio of IC<sub>50</sub> without a modulator to IC<sub>50</sub> with a modulator. Alone, **5a**, **9a**, and **11a** weakly inhibited *ABCB1*/Flp-In<sup>TM</sup>-293 cell growth (<10%) at 8 and 10 μM. Preliminarily, we found that *ABCB1*/Flp-In<sup>TM</sup>-293 cells were about 1196.9, 137.9 and 9.9-fold more resistant toward paclitaxel, vincristine, and doxorubicin than their parental Flp-In<sup>TM</sup>-293 cells, respectively. Then the MDR-reversal activity of the studied compounds was tested using the same method in the presence of paclitaxel, vincristine, or doxorubicin (**Table 3**). For paclitaxel cytotoxicity, **5a** (RF = 16.1) exhibited a higher modulating activity than **9a** (RF = 8.2) and **11a** (RF= 9.5) at 10 μM. For vincristine cytotoxicity, **5a** (RF = 21.0) exhibited a greater modulating activity than **9a** (RF = 1.6) and **11a** (RF= 9.7) at 10 μM. For doxorubicin cytotoxicity, **5a** (RF = 1.6), **9a** (RF = 1.7) and **11a** (RF= 1.5) at 10 μM were roughly equal in their ability to reverse doxorubicin resistance in *ABCB1*/Flp-In<sup>TM</sup>-293 cells.

**Table 3** herein

Furthermore, the MDR cancer cell line KBvin and the parental cancer cell line HeLaS3 were employed in this study (**Table 4**). For paclitaxel cytotoxicity, **5a** displayed a potent P-gp modulating activity with a RF of 23.1 at 10 μM. For vincristine cytotoxicity, **5a** displayed a powerful reversal activity with RF of 29.7 at 10 μM. Additionally, **5a** at 10 μM with vincristine co-administered showed a moderate modulating activity with a RF of 8.8 in the parental cancer cell line HeLaS3.

**Table 4** herein

### 2.2.3. *ABCB1* mRNA detected by RT-qPCR

In the *ABCB1* mRNA, expression was detected by real-time quantitative reverse transcription PCR (**Figure 3**). **5a** and **11a** significantly decreased *ABCB1* mRNA expression in the P-gp-transfected cell line *ABCB1*/Flp-In<sup>TM</sup>-293. **9a** showed no effect on *ABCB1* mRNA expression level in both the P-gp-transfected cell line *ABCB1*/Flp-In<sup>TM</sup>-293 and its parental cell line Flp-In<sup>TM</sup>-293, while little *ABCB1* gene expression was detected in the parental cell line Flp-In<sup>TM</sup>-293.

**Figure 3** herein

#### 2.2.4. Docking interaction of compound **5a** and **5b** with P-gp.

The compound **5a** and **5b** was docked into the binding site of drug binding domain (DBD) to provide the interaction between the ligand and the receptor (**Figure 4a, 4b**). Docking was done using Discovery Studio 3.1 software. Remarkably, **5a** is stabilized through specific interactions such as hydrogen bonding with residues in the drug binding domain of P-gp and nonspecific interactions such as hydrophobic  $\pi - \pi$  stacking aromatic interactions. The hydrogen bond acceptor oxygen atom at the 1, 5, and 10-position of the benzodipyranone-4,10-dione showed hydrogen bonding interaction with the side chain of TYR306 and SER725, respectively. The hydrogen bond donor at the 5-position of the hydroxy group showed hydrogen bonding interaction with the side chain of the SER725. The phenyl rings of the 3-*m*-tolyl group interacted with PHE71 and PHE728 through  $\pi - \pi$  stacking aromatic interactions. However, compound **5b** only generated a hydrogen bond interaction with TYR306. These results were verified our SAR deduction that benzodipyranone-4,10-dione **4a-31a** have a higher degree of reaching a conformation that is high affinity for matching the drug binding sites of P-gp than the corresponding benzodipyranone-4,6-dione **4b-31b**.

**Figure 4** herein

### 3. Conclusion

In this study, we synthesized a novel series of benzodipyranone derivatives and evaluated their inhibitory activity of P-gp by the *ABCBI/Flp-In*<sup>TM</sup>-293 cell line fluorescence efflux of a specific P-gp substrate Calcein-AM. The structure activity relationship (SAR) study suggests that asymmetrical benzodipyranone-4,10-dione **4a-31a** bearing on the R substituents with electron donating group exhibited a better inhibitory activity of P-gp efflux function (between 1.53 to 2.05 fold) than electron withdrawing substituents at 5  $\mu$ M. These results illustrate that the substituent of an electron donating group play an important factor in determining P-gp inhibitory activity. However, the symmetrical benzodipyranone-4,6-dione **4b-31b** were inactive toward P-gp inhibitory effect. According to the SAR and molecule docking results, the benzodipyranone-4,10-dione derivatives (**4a-31a**) have a higher degree of reaching a conformation that is more suitable for matching with the drug-binding pocket of P-gp than the corresponding benzodipyranone-4,6-dione derivatives (**4b-31b**). At the higher dose tested (10  $\mu$ M), **5a**, **9a**, and **11a** were able to significantly ( $p < 0.05$ ) reverse paclitaxel, vincristine, and doxorubicin resistance. **5a** was the most potent compound

in that it significantly sensitized *ABCB1*/Flp-In<sup>TM</sup>-293 cells to various anticancer drugs including paclitaxel, vincristine, and doxorubicin with nanomolar IC<sub>50</sub> values (IC<sub>50</sub> ranged from 39.11 to 586.26 nM). In addition, **5a** at 10 μM was able to sensitize MDR cell line KBvin toward paclitaxel and vincristine by 23.1-fold and 29.7-fold, respectively.

The present study demonstrates that these synthetic derivatives of benzodipyrone derivatives can be employed as effective inhibitors of P-gp mediated drug resistance in cancer cells, and their mechanism of MDR inhibition is associated with an increasing intracellular accumulation of a given anticancer drug induced by directly blocking P-gp-mediated drug efflux or reducing *ABCB1* mRNA expression level. In conclusion, we have defined the structure-activity relationships of these new series of P-gp inhibitors and identified **5a** as having a good efficacy, which might prove useful down the line as a lead for the development of new inhibitors of P-gp-mediated MDR.

## 4. Experimental section

### 4.1. Chemistry

#### 4.1.1. Materials and methods

Reagents and solvents were obtained commercially and used without further purification. Reactions were monitored by TLC, using Merck plates with fluorescent indicator (TLC Silica Gel 60 F<sub>254</sub>). Flash column chromatography was performed on silica gel (Merck Silica Gel 60, 400-630 mesh). Melting points were determined on a Yanaco MP-500D melting point apparatus and were uncorrected. <sup>1</sup>H and <sup>13</sup>C NMR spectra were obtained on a Bruker Ultrashield 500 plus FT-NMR Spectrometer (500 MHz) in DMSO-*d*<sub>6</sub>. The following abbreviations are used: s, singlet; d, doublet; t, triplet; m, multiplet. EI-HRMS and EIMS were measured with a Finnigan/Thermo Quest MAT 95XL instrument, ESIMS was measured with a Finnigan/Thermo LCQ ion-trap mass spectrometer. The purity of active compounds was assessed using a HPLC. The column used was a C18 reverse phase column (NUCLEODUR C18 HTec, 250 mm × 4.6 mm, 5 μm) attached to a Jasco 851-AS autosample and Jasco PU-980 pump coupled to a Jasco MD-910 photodiode array (PDA) detector was used. Each sample was injected at a volume of 20 μL and eluted with an isocratic mobile phase (methanol/water), and the flow rate was 1 mL/min. All tested compounds were confirmed to be ≥ 97% pure based on the area of the major peak when compared to the total combined area. Note: compound **19a**, **21a**, **23a**, **24a**, **25a**, **26a**, **6b**, **9b**, **15b**, **16b**, **18b**, **19b**, **24b**, **25b**, and **27b** difficult to dissolve in DMSO, DMF and pyridine,

so it is unable to obtain  $^{13}\text{C}$  NMR spectrum.

#### 4.1.2. General procedure for synthesis of benzodipyrone derivatives **4a,b-31a,b**

To a solution of phloroglucinol (**1**, 1 mmol) and appropriate acetonitrile (**2**, 2.4 mmol) dissolved in borontrifluoride etherate (15 mL) was purged HCl gas. The mixture was stirred at room temperature for 10-14 h followed by the addition of 1 M HCl (15 mL). The resulting mixture was stirred at reflux for 4 h, and after completion as monitored by TLC, the reaction residue was diluted with ethyl acetate. The ethyl acetate layer was then washed with saturated  $\text{NaHCO}_3$  aqueous and brine. The organic fractions were dried over anhydrous  $\text{MgSO}_4$  and evaporated under vacuum. The residue was purified by flash chromatography on silica gel using ethyl acetate–dichloromethane as eluent to provide corresponding products **3**.

A mixture of the appropriate **3** (1 mmol), methanesulfonyl chloride (6 mmol) and DMF (6 mmol) in borontrifluoride etherate (1 mL) was stirred at 120 °C for 2-4 h. After reaction completion as monitored by TLC, the resulting mixture was cooled at 60 °C with vigorous stir, and the reaction mixture was diluted with ethyl acetate, the suspension was filtered and the solid washed with ethyl acetate to afford symmetrical benzodipyrano-4,6-dione **4b-31b** as a solid. Subsequently, the filtrate was then washed with 1 M HCl and brine. The organic fractions were dried over anhydrous  $\text{MgSO}_4$  and evaporated under vacuum. The residue was subjected to flash chromatography on silica gel used a mixture of ethyl acetate–*n*-hexane as eluent to provide asymmetrical benzodipyrano-4,10-dione **4a-31a**.

#### 4.1.3. 5-hydroxy-3,9-di-*o*-tolylpyrano[2,3-*f*]chromene-4,10-dione (**4a**)

Orange solid. Yield 8%. mp 111.1-111.8 °C;  $^1\text{H}$  NMR (500 MHz,  $\text{DMSO-}d_6$ )  $\delta$  13.78 (s, 1 H, OH), 8.66 (s, 1 H, 2-H), 8.28 (s, 1 H, 8-H), 7.04-7.37 (m, 8 H, ArH), 5.74 (s, 1 H, 6-H), 2.21 (s, 3 H,  $\text{CH}_3$ ), 2.18 (s, 3 H,  $\text{CH}_3$ );  $^{13}\text{C}$  NMR (125 MHz,  $\text{DMSO-}d_6$ )  $\delta$  180.3, 172.5, 163.9, 161.5, 156.7, 156.2, 152.7, 137.6, 131.5, 130.7, 130.6, 129.8, 129.8, 129.7, 128.7, 128.3, 126.7, 125.7, 125.6, 125.4, 108.8, 106.6, 99.5, 99.5, 19.6, 19.5. EIMS  $m/z$  410.2 ( $\text{M}^+$ ). HPLC purity 99.8% ( $\lambda_{\text{max}}$  280 nm).

#### 4.1.4. 5-hydroxy-3,9-di-*m*-tolylpyrano[2,3-*f*]chromene-4,10-dione (**5a**)

Yellow solid. Yield 33%. mp 146.5-147-2 °C;  $^1\text{H}$  NMR (500 MHz,  $\text{DMSO-}d_6$ )  $\delta$  13.84 (s, 1 H, OH), 8.78 (s, 1 H, 2-H), 8.40 (s, 1 H, 8-H), 7.40-7.44 (m, 2 H, 6,; 6''-H), 7.30-7.37 (m, 4 H, 2', 4', 2'', 4''-H), 7.20-7.25 (m, 2 H, 5', 5''-H), 6.97 (s, 1 H, 6-H), 2.36 (s, 3 H,  $\text{CH}_3$ ), 2.35 (s, 3 H,  $\text{CH}_3$ );  $^{13}\text{C}$  NMR (125MHz,  $\text{DMSO-}d_6$ )  $\delta$  180.4, 172.6, 163.9, 161.2, 156.0, 155.9, 152.2, 137.4, 137.2, 131.2, 129.7, 129.6, 129.5, 129.1, 128.6, 128.2, 128.0, 126.1, 126.1, 125.4, 124.4, 108.9, 106.5, 99.4, 21.0, 21.0. EIMS

$m/z$  410.2 ( $M^+$ ). HPLC purity 99.6% ( $\lambda_{\max}$  280 nm).

#### 4.1.5. 5-hydroxy-3,9-di-*p*-tolylpyrano[2,3-*f*]chromene-4,10-dione (6a)

White solid. Yield 19%. mp 202.5-203.1 °C;  $^1\text{H}$  NMR (500 MHz,  $\text{DMSO-}d_6$ )  $\delta$  13.85 (s, 1 H, OH), 8.78 (s, 1 H, 2-H), 8.37 (s, 1 H, 8-H), 7.52 (d,  $J = 8.1$  Hz, 2 H, 2', 6'-H), 7.43 (d,  $J = 8.1$  Hz, 2 H, 2'', 6''-H), 7.27 (d,  $J = 8.0$  Hz, 2 H, 3', 5'-H), 7.23 (d,  $J = 8.0$  Hz, 2 H, 3'', 5''-H), 6.95 (s, 1 H, 6-H), 2.35 (d,  $J = 5.3$  Hz, 6 H, 4', 2 $\times$ CH<sub>3</sub>);  $^{13}\text{C}$  NMR (125MHz,  $\text{DMSO-}d_6$ )  $\delta$  180.5, 172.7, 163.9, 161.2, 156.0, 155.9, 152.0, 138.0, 137.3, 128.9, 128.9, 128.8, 128.8, 128.7, 128.7, 128.3, 126.9, 125.2, 124.2, 108.9, 106.5, 99.3, 99.3, 20.8, 20.8, 20.8. EIMS  $m/z$  410.1 ( $M^+$ ). HPLC purity 99.3% ( $\lambda_{\max}$  252 nm).

#### 4.1.6. 5-hydroxy-3,9-bis(2-methoxyphenyl)pyrano[2,3-*f*]chromene-4,10-dione (7a)

Brown powder. Yield 16%. mp 216.8-217.6 °C;  $^1\text{H}$  NMR (500 MHz,  $\text{DMSO-}d_6$ )  $\delta$  13.81 (s, 1 H, OH), 8.65 (s, 1 H, 2-H), 8.25 (s, 1 H, 8-H), 7.38-7.45 (m, 2 H, ArH), 7.32 (dd,  $J = 1.6, 7.5$  Hz, 1 H, ArH), 7.24 (dd,  $J = 1.6, 7.4$  Hz, 1 H, ArH), 7.13 (d,  $J = 8.2$  Hz, 1 H, ArH), 7.09 (d,  $J = 8.1$  Hz, 1 H, ArH), 7.00-7.05 (m, 2 H, ArH), 6.98 (s, 1 H, 6-H), 3.76 (s, 3 H, OCH<sub>3</sub>), 3.73 (s, 3 H, OCH<sub>3</sub>);  $^{13}\text{C}$  NMR (125 MHz,  $\text{DMSO-}d_6$ )  $\delta$  180.2, 172.3, 163.8, 161.4, 157.5, 157.4, 156.8, 156.0, 152.5, 131.6, 131.5, 130.4, 129.9, 124.0, 122.5, 120.5, 120.3, 120.2, 118.7, 111.5, 111.3, 108.7, 106.5, 99.5, 55.7, 55.6. EIMS  $m/z$  442.1 ( $M^+$ ). HPLC purity 99.3% ( $\lambda_{\max}$  272 nm).

#### 4.1.7. 5-hydroxy-3,9-bis(3-methoxyphenyl)pyrano[2,3-*f*]chromene-4,10-dione (8a)

White powder. Yield 23%. mp 185.9-186.8 °C;  $^1\text{H}$  NMR (500 MHz,  $\text{DMSO-}d_6$ )  $\delta$  13.84 (s, 1 H, OH), 8.84 (s, 1 H, 2-H), 8.43 (s, 1 H, 8-H), 7.37-7.40 (m, 1 H, 5'-H), 7.33-7.36 (m, 1 H, 5''-H), 7.21-7.22 (m, 2 H, 2', 4'-H), 7.11-7.14 (m, 2 H, 2'', 4''-H), 7.01 (dd,  $J = 2.1, 8.3$  Hz, 1 H, 6'-H), 6.98 (s, 1 H, 6-H), 6.96 (dd,  $J = 2.1, 8.3$  Hz, 1 H, 6''-H), 3.80 (s, 3 H, OCH<sub>3</sub>), 3.79 (s, 3 H, OCH<sub>3</sub>);  $^{13}\text{C}$  NMR (125MHz,  $\text{DMSO-}d_6$ )  $\delta$  180.4, 172.5, 164.0, 161.1, 159.1, 159.0, 156.3, 155.9, 152.5, 132.6, 131.1, 129.4, 129.1, 125.1, 124.1, 121.2, 121.2, 114.6, 114.6, 114.0, 113.7, 108.9, 106.6, 99.4, 55.1, 55.1. EIMS  $m/z$  442.1 ( $M^+$ ).

#### 4.1.8. 5-hydroxy-3,9-bis(4-methoxyphenyl)pyrano[2,3-*f*]chromene-4,10-dione (9a)

Brown powder. Yield 39%. mp 163.2-164.0 °C;  $^1\text{H}$  NMR (500 MHz,  $\text{DMSO-}d_6$ )  $\delta$  13.89 (s, 1 H, OH), 8.78 (s, 1 H, 2-H), 8.37 (s, 1 H, 8-H), 7.59 (d,  $J = 8.5$  Hz, 2 H, 2', 6'-H), 7.50 (d,  $J = 8.5$  Hz, 2 H, 2'', 6''-H), 7.03 (d,  $J = 8.5$  Hz, 2 H, 3', 5'-H), 7.00 (d,  $J = 8.5$  Hz, 2 H, 3'', 5''-H), 6.96 (s, 1 H, 6-H), 3.80 (s, 3 H, OCH<sub>3</sub>), 3.80 (s, 3 H, OCH<sub>3</sub>);  $^{13}\text{C}$  NMR (125MHz,  $\text{DMSO-}d_6$ )  $\delta$  180.6, 172.9, 163.9, 161.2, 159.5, 159.2,

156.0, 155.5, 151.7, 130.3, 130.3, 130.2, 130.2, 125.0, 123.9, 123.4, 121.9, 113.8, 113.8, 113.6, 113.6, 108.8, 106.6, 99.3, 55.2, 55.1. EIMS  $m/z$  442.1 ( $M^+$ ). HPLC purity 97.6% ( $\lambda_{\max}$  248 nm).

4.1.9. *5-hydroxy-3,9-bis(3-hydroxyphenyl)pyrano[2,3-f]chromene-4,10-dione (10a)*

Pale-yellow crystal. Yield 22%. mp 305.2-306.0 °C;  $^1\text{H}$  NMR (500 MHz, DMSO- $d_6$ )  $\delta$  13.88 (s, 1 H, 5-OH), 9.56 (s, 1 H, 3'-OH), 9.47 (s, 1 H, 3''-OH), 8.77 (s, 1 H, 2-H), 8.38 (s, 1 H, 8-H), 7.25 (t,  $J = 7.9$  Hz, 1 H, 5'-H), 7.22 (t,  $J = 7.9$  Hz, 1 H, 5''-H), 7.20-7.27 (m, 2 H, ArH), 6.93-7.06 (m, 5 H, ArH), 6.78-6.84 (m, 2 H, ArH);  $^{13}\text{C}$  NMR (125 MHz, DMSO- $d_6$ )  $\delta$  180.4, 172.6, 164.0, 161.1, 157.1, 157.0, 156.1, 156.0, 152.2, 132.5, 131.0, 129.3, 129.1, 125.4, 124.3, 119.6, 119.6, , 116.1, 115.5, 115.0, 108.9, 106.6, 99.3, 99.3. EIMS  $m/z$  414.1 ( $M^+$ ).

4.1.10. *3,9-bis(3,4-dimethoxyphenyl)-5-hydroxypyran[2,3-f]chromene-4,10-dione (11a)*

Brown solid. Yield 6%. mp 149.1-149.9 °C;  $^1\text{H}$  NMR (500 MHz, DMSO- $d_6$ )  $\delta$  13.91 (s, 1 H, OH), 8.84 (s, 1 H, 2-H), 8.40 (s, 1 H, 8-H), 7.26 (d,  $J = 1.5$  Hz, 1 H, 2'-H), 7.23 (dd,  $J = 1.5, 8.3$  Hz, 1 H, 5'-H), 7.19 (d,  $J = 1.5$  Hz, 1 H, 2''-H), 7.11 (dd,  $J = 1.5, 8.3$  Hz, 1 H, 5''-H), 7.05 (d,  $J = 8.35$  Hz, 1 H, 6'-H), 7.01 (d,  $J = 8.3$  Hz, 1 H, 6''-H), 6.96 (s, 1 H, 6-H), 3.80 (s, 6 H, OCH<sub>3</sub>), 3.79 (s, 6 H, OCH<sub>3</sub>);  $^{13}\text{C}$  NMR (125 MHz, DMSO- $d_6$ )  $\delta$  180.6, 172.8, 163.9, 161.1, 155.9, 155.8, 151.9, 149.2, 148.8, 148.4, 148.3, 125.0, 124.0, 123.7, 122.2, 121.5, 121.3, 112.9, 112.7, 111.7, 111.5, 108.8, 106.5, 99.3, 55.6, 55.6, 55.6, 55.6. EIMS  $m/z$  502.2 ( $M^+$ ). HPLC purity 99.3% ( $\lambda_{\max}$  212 nm).

4.1.11. *5-hydroxy-3,9-bis(3,4,5-trimethoxyphenyl)pyrano[2,3-f]chromene-4,10-dione (12a)*

White solid. Yield 20%. mp 268.0-268.7 °C;  $^1\text{H}$  NMR (500 MHz, DMSO- $d_6$ )  $\delta$  13.87 (s, 1 H, OH), 8.89 (s, 1 H, 2-H), 8.46 (s, 1 H, 8-H), 6.98 (s, 3 H, 6, 2', 6'-H), 6.89 (s, 2 H, 2'', 6''-H), 3.81 (s, 6 H, 2xOCH<sub>3</sub>), 3.80 (s, 6 H, 2xOCH<sub>3</sub>), 3.70 (s, 3 H, OCH<sub>3</sub>), 3.69 (s, 3 H, OCH<sub>3</sub>);  $^{13}\text{C}$  NMR (125 MHz, DMSO- $d_6$ )  $\delta$  180.3, 172.6, 164.0, 161.1, 156.3, 155.9, 152.7, 152.5, 152.5, 152.5, 152.5, 137.8, 137.5, 126.7, 125.3, 125.1, 124.0, 108.9, 106.6, 106.6, 106.6, 106.6, 106.5, 99.4, 60.0, 60.0, 56.0, 56.0, 55.9, 55.9. EIMS  $m/z$  562.1 ( $M^+$ ).

4.1.12.

*3,9-bis(benzo[d][1,3]dioxol-5-yl)-5-hydroxypyran[2,3-f]chromene-4,10-dione (13a)*

Yellow solid. Yield 64%. mp 350.5-351.4 °C;  $^1\text{H}$  NMR (500 MHz, DMSO- $d_6$ )  $\delta$

13.63 (s, 1 H, OH), 8.70 (s, 1 H, 2-H), 8.30 (s, 1 H, 8-H), 7.21 (d,  $J = 1.6$  Hz, 1 H, 2'-H), 7.16 (dd,  $J = 1.6, 8.1$  Hz, 1 H, 6'-H), 7.13 (d,  $J = 1.6$  Hz, 1 H, 2''-H), 7.06 (dd,  $J = 1.6, 8.0$  Hz, 1 H, 6''-H), 6.99 (d,  $J = 8.1$  Hz, 1 H, 5'-H), 6.95 (d,  $J = 8.0$  Hz, 1 H, 5''-H), 6.90 (s, 1 H, 6-H), 6.05 (s, 2 H, CH<sub>2</sub>), 6.04 (s, 2 H, CH<sub>2</sub>); <sup>13</sup>C NMR (125 MHz, DMSO-*d*<sub>6</sub>)  $\delta$  180.1, 172.3, 163.6, 160.9, 155.6, 155.2, 151.4, 147.2, 146.9, 146.8, 146.7, 124.8, 124.6, 123.8, 123.1, 122.4, 122.2, 109.1, 109.0, 108.6, 107.8, 107.6, 106.3, 100.8, 100.7, 98.9. EIMS  $m/z$  470.0 (M<sup>+</sup>).

4.1.13. *3,9-bis(2-fluorophenyl)-5-hydroxypyrano[2,3-f]chromene-4,10-dione (14a)*

White solid. Yield 13%. mp 234.3-235.2 °C; <sup>1</sup>H NMR (500 MHz, DMSO-*d*<sub>6</sub>)  $\delta$  13.6 (s, 1 H, OH), 8.83 (s, 1 H, 2-H), 8.45 (s, 1 H, 8-H), 7.43-7.55 (m, 4 H, 3', 5', 3'', 5''-H), 7.27-7.36 (m, 4 H, 4', 6', 4'', 6''-H), 7.06 (s, 1 H, 6-H); <sup>13</sup>C NMR (125 MHz, DMSO-*d*<sub>6</sub>)  $\delta$  179.6, 171.7, 163.9, 161.4, 160.1 (d,  $J = 245.4$  Hz, 1 C), 160.0 (d,  $J = 245.1$  Hz, 1 C), 157.3, 156.0, 153.4, 132.2, 132.1 (d,  $J = 2.75$  Hz, 1 C), 131.1 (d,  $J = 8.1$  Hz, 1 C), 130.6 (d,  $J = 8.0$  Hz, 1 C), 124.4 (d,  $J = 19.6$  Hz, 1 C), 124.4 (d,  $J = 19.8$  Hz, 1 C), 121.6, 120.3, 119.3 (d,  $J = 15.5$  Hz, 1 C), 117.7 (d,  $J = 15.6$  Hz, 1 C), 115.6 (d,  $J = 19.5$  Hz, 1 C), 115.4 (d,  $J = 21.3$  Hz, 1 C), 108.0, 106.4, 99.8. EIMS  $m/z$  418.1 (M<sup>+</sup>).

4.1.14. *3,9-bis(3-fluorophenyl)-5-hydroxypyrano[2,3-f]chromene-4,10-dione (15a)*

Brown solid. Yield 27%. mp 240.9-241.8 °C; <sup>1</sup>H NMR (500 MHz, DMSO-*d*<sub>6</sub>)  $\delta$  13.72 (s, 1 H, OH), 8.89 (s, 1 H, 2-H), 8.51 (s, 1 H, 8-H), 7.45-7.54 (m, 4 H, 2', 2'', 4', 4''-H), 7.40-7.43 (m, 2 H, 6', 6''-H), 7.21-7.30 (m, 2 H, 5', 5''-H), 7.00 (s, 1 H, 6-H); <sup>13</sup>C NMR (125 MHz, DMSO-*d*<sub>6</sub>)  $\delta$  180.1, 172.3, 164.0, 161.8 (d,  $J = 241.6$  Hz, 1 C), 161.8 (d,  $J = 241.1$  Hz, 1 C), 161.1, 156.7, 155.8, 153.1, 133.6 (d,  $J = 8.6$  Hz, 1 C), 132.1 (d,  $J = 8.5$  Hz, 1 C), 130.3 (d,  $J = 8.4$  Hz, 1 C), 130.0 (d,  $J = 8.4$  Hz, 1 C), 125.0 (d,  $J = 2.6$  Hz, 1 C), 125.0 (d,  $J = 2.1$  Hz, 1 C), 124.0, 123.0, 115.8 (d,  $J = 22.4$  Hz, 2 C), 115.3 (d,  $J = 20.8$ , 1 C), 114.8 (d,  $J = 20.5$  Hz, 1 C), 108.9, 106.5, 99.6, 99.6. EIMS  $m/z$  418.1 (M<sup>+</sup>).

4.1.15. *3,9-bis(4-fluorophenyl)-5-hydroxypyrano[2,3-f]chromene-4,10-dione (16a)*

Pale-brown solid. Yield 23%. mp 273.8-274.5 °C; <sup>1</sup>H NMR (500 MHz, DMSO-*d*<sub>6</sub>)  $\delta$  13.77 (s, 1 H, OH), 8.83 (s, 1 H, 2-H), 8.44 (s, 1 H, 8-H), 7.67-7.70 (m, 2 H, 3', 5'-H), 7.58-7.61 (m, 2 H, 3'', 5''-H), 7.31 (t,  $J = 8.9$  Hz, 2 H, 2', 6'-H), 7.27 (t,  $J = 8.9$  Hz, 2 H, 2'', 6''-H), 6.99 (s, 1 H, 6-H); <sup>13</sup>C NMR (125 MHz, DMSO-*d*<sub>6</sub>)  $\delta$  180.3, 172.6, 164.0, 162.2 (d,  $J = 244.8$  Hz, 1 C), 162.0 (d,  $J = 243.4$  Hz, 1 C), 156.2, 156.0, 152.5, 131.2 (d, 7.8 Hz, 2 C), 131.2 (d,  $J = 7.9$  Hz, 2 C), 127.6 (d,  $J = 2.8$  Hz, 1 C), 126.2 (d,  $J = 2.63$  Hz, 1 C), 124.4, 123.4, 115.3 (d,  $J = 21.4$  Hz, 2 C), 115.0 (d,  $J =$

21.1 Hz, 2 C) 109.0, 106.5, 99.5, 99.5. EIMS  $m/z$  418.0 ( $M^+$ ).

4.1.16. *3,9-bis(2-chlorophenyl)-5-hydroxypyrano[2,3-f]chromene-4,10-dione (17a)*

White powder. Yield 22%. mp 197.9-198.8 °C;  $^1\text{H}$  NMR (500 MHz, DMSO- $d_6$ )  $\delta$  13.58 (s, 1 H, OH), 8.78 (s, 1 H, 2-H), 8.40 (s, 1 H, 8-H), 7.61 (d,  $J = 7.6$  Hz, 1 H, 3'-H), 7.61 (d,  $J = 7.7$  Hz, 1 H, 3''-H), 7.42-7.52 (m, 6 H, 4', 5', 6', 4'', 5'', 6''-H), 7.08 (s, 1 H, 6-H);  $^{13}\text{C}$  NMR (125MHz, DMSO- $d_6$ )  $\delta$  179.6, 171.7, 163.9, 161.5, 157.3, 156.0, 153.3, 133.9, 133.8, 132.6, 132.5, 130.8, 130.7, 130.2, 129.3, 129.3, 129.2, 127.2, 127.1, 125.0, 123.7, 108.8, 106.5, 99.9. EIMS  $m/z$  415 (M-36).

4.1.17. *3,9-bis(3-chlorophenyl)-5-hydroxypyrano[2,3-f]chromene-4,10-dione (18a)*

White solid. Yield 46%. mp 201.5-202.0 °C;  $^1\text{H}$  NMR (500 MHz, DMSO- $d_6$ )  $\delta$  13.68 (s, 1 H, OH), 8.88 (s, 1 H, 2-H), 8.51 (s, 1 H, 8-H), 7.72 (d,  $J = 0.7$  Hz, 1 H, 2'-H), 7.63 (d,  $J = 0.7$  Hz, 1 H, 2''-H), 7.59 (m, 1 H, ArH), 7.48-7.52 (m, 3 H, ArH), 7.45-7.46 (m, 2 H, 6', 6''-H), 6.99 (s, 1 H, 6-H);  $^{13}\text{C}$  NMR (125 MHz, DMSO- $d_6$ )  $\delta$  180.0, 172.3, 164.0, 161.1, 156.7, 155.9, 153.1, 133.4, 133.0, 132.7, 132.0, 130.2, 130.0, 128.7, 128.7, 128.4, 127.9, 127.6, 127.6, 123.9, 123.0, 108.9, 106.4, 99.6. EIMS  $m/z$  450.0 ( $M^+$ ).

4.1.18. *3,9-bis(4-chlorophenyl)-5-hydroxypyrano[2,3-f]chromene-4,10-dione (19a)*

Pale-brown solid. Yield 18%. mp 306.8-307.6 °C;  $^1\text{H}$  NMR (500 MHz, DMSO- $d_6$ )  $\delta$  13.74 (s, 1 H, OH), 8.87 (s, 1 H, 2-H), 8.48 (s, 1 H, 8-H), 7.68 (d,  $J = 8.5$  Hz, 2 H, 3', 5'-H), 7.59 (d,  $J = 8.5$  Hz, 2 H, 3'', 5''-H), 7.55 (d,  $J = 8.5$  Hz, 2 H, 2', 6'-H), 7.51 (d,  $J = 8.5$  Hz, 2 H, 2'', 6''-H), 7.02 (s, 1 H, 6-H). EI-HRMS  $m/z$  450.0070 ( $M^+$ ), calcd for  $\text{C}_{24}\text{H}_{12}\text{Cl}_2\text{O}_5$ : 450.0062.

4.1.19. *5-hydroxy-3,9-bis(2-nitrophenyl)pyrano[2,3-f]chromene-4,10-dione (20a)*

White solid. Yield 35%. mp 307.9-308.7 °C;  $^1\text{H}$  NMR (500 MHz, DMSO- $d_6$ )  $\delta$  13.25 (s, 1 H, OH), 8.96 (s, 1 H, 2-H), 8.64 (s, 1 H, 8-H), 8.18 (d,  $J = 8.1$  Hz, 1 H, 3'-H), 8.13 (d,  $J = 8.1$  Hz, 1 H, 3''-H), 7.84-7.91 (m, 2 H, 5', 5''-H), 7.71-7.77 (m, 2 H, 4', 4''-H), 7.67 (d,  $J = 7.3$  Hz, 1 H, 6'-H), 7.62 (d,  $J = 7.3$  Hz, 1 H, 6''-H), 7.12 (s, 1 H, 6-H);  $^{13}\text{C}$  NMR (125 MHz, DMSO- $d_6$ )  $\delta$  179.1, 171.5, 163.9, 161.6, 156.1, 155.9, 152.2, 149.1, 148.8, 134.2, 133.9, 132.8, 132.5, 130.5, 130.0, 125.7, 124.8, 124.5, 124.3, 124.3, 123.7, 108.2, 105.8, 100.0. EIMS  $m/z$  426.1 (M-46).

4.1.20. *5-hydroxy-3,9-bis(4-nitrophenyl)pyrano[2,3-f]chromene-4,10-dione (21a)*

Brown solid. Yield 77%. mp 343.7-344.5 °C;  $^1\text{H}$  NMR (500 MHz, DMSO- $d_6$ )  $\delta$  13.65 (s, 1 H, OH), 9.03 (s, 1 H, 2-H), 8.66 (s, 1 H, 8-H), 8.34 (d,  $J = 8.7$  Hz, 2 H, 3',

5'-H), 8.31 (d,  $J = 8.7$  Hz, 2 H, 3'', 5''-H), 7.96 (d,  $J = 8.7$  Hz, 2 H, 2', 6'-H), 7.90 (d,  $J = 8.7$  Hz, 2 H, 2'', 6''-H), 7.11 (s, 1 H, 6-H). EI-HRMS  $m/z$  472.0546 ( $M^+$ ), calcd for  $C_{24}H_{12}N_2O_9$ : 472.0543.

4.1.21. *3,9-bis(2-chloro-6-fluorophenyl)-5-hydroxypyrano[2,3-f]chromene-4,10-dione (22a)*

Yellow solid. Yield 22%. mp 196.3-197.2 °C;  $^1H$  NMR (500 MHz, DMSO- $d_6$ )  $\delta$  13.65 (s, 1 H, OH), 8.93 (s, 1 H, 2-H), 8.55 (s, 1 H, 8-H), 7.47-7.60 (m, 4 H, 3', 5', 3'', 5''-H), 7.35-7.41 (m, 2 H, 4', 4''-H), 7.12 (s, 1 H, 6-H);  $^{13}C$  NMR (125 MHz, DMSO- $d_6$ )  $\delta$  179.0, 171.2, 163.9, 161.5, 160.7 (d,  $J = 246.0$  Hz, 1 C), 160.6 (d,  $J = 246.4$  Hz, 1 C), 158.6, 156.0, 154.7, 135.0 (d,  $J = 13.5$  Hz, 1 C), 135.0 (d,  $J = 13.5$  Hz, 1 C), 131.9 (d,  $J = 9.5$  Hz, 1 C), 131.4 (d,  $J = 9.4$  Hz, 1 C), 125.4 (d,  $J = 1.5$  Hz, 1 C), 125.2 (d,  $J = 1.6$  Hz, 1 C), 118.9 (d,  $J = 19.6$  Hz, 1 C), 118.8, 117.6, 117.4 (d,  $J = 19.4$  Hz, 1 C), 114.5 (d,  $J = 21.8$  Hz, 1 C), 114.4 (d,  $J = 22.0$  Hz, 1 C), 108.8, 106.4, 100.3. EIMS  $m/z$  451 ( $M-36$ ).

4.1.22. *3,9-bis(3,4-dichlorophenyl)-5-hydroxypyrano[2,3-f]chromene-4,10-dione (23a)*

White solid. Yield 8%. mp 326.2-327.1 °C;  $^1H$  NMR (500 MHz, DMSO- $d_6$ )  $\delta$  13.63 (s, 1 H, OH), 8.93 (s, 1 H, 2-H), 8.57 (s, 1 H, 8-H), 7.94 (d,  $J = 2.0$  Hz, 1 H, 2'-H), 7.86 (d,  $J = 2.0$  Hz, 1 H, 2''-H), 7.75 (d,  $J = 8.4$  Hz, 1 H, 5'-H), 7.71 (d,  $J = 8.4$  Hz, 1 H, 5''-H), 7.65 (dd,  $J = 2.0, 8.4$  Hz, 1 H, 6'-H), 7.58 (dd,  $J = 2.0, 8.4$  Hz, 1 H, 6''-H), 7.04 (s, 1 H, 6-H). EI-HRMS  $m/z$  517.9286 ( $M^+$ ), calcd for  $C_{24}H_{10}Cl_4O_5$ : 517.9282.

4.1.23.

*5-hydroxy-3,9-bis(2-(trifluoromethyl)phenyl)pyrano[2,3-f]chromene-4,10-dione (24a)*

White solid. Yield 26%. mp 118.7-119.5 °C;  $^1H$  NMR (500 MHz, DMSO- $d_6$ )  $\delta$  13.47 (s, 1 H, OH), 8.74 (s, 1 H, 2-H), 8.37 (s, 1 H, 8-H), 7.88 (d,  $J = 7.8$  Hz, 1 H, 6'-H), 7.85 (d,  $J = 7.8$  Hz, 1 H, 6''-H), 7.67-7.78 (m, 4 H, 3', 5', 3'', 5''-H), 7.56 (d,  $J = 7.6$  Hz, 1 H, 4'-H), 7.48 (d,  $J = 7.6$  Hz, 1 H, 4''-H), 7.08 (s, 1 H, 6-H). EI-HRMS  $m/z$  518.0585 ( $M^+$ ), calcd for  $C_{26}H_{12}F_6O_5$ : 518.0589.

4.1.24.

*5-hydroxy-3,9-bis(3-(trifluoromethyl)phenyl)pyrano[2,3-f]chromene-4,10-dione (25a)*

White crystal. Yield 48%. mp 212.6-213.3 °C;  $^1H$  NMR (500 MHz, DMSO- $d_6$ )  $\delta$  13.65 (s, 1 H, 5-OH), 8.95 (s, 1 H, 2-H), 8.58 (s, 1 H, 8-H), 8.03 (s, 1 H, 2'-H), 7.95 (s,

1 H, 2''-H), 7.93 (d,  $J=7.8$  Hz, 1 H, 4'-H), 7.85 (d,  $J=7.8$  Hz, 1 H, 6'-H), 7.80 (d,  $J=7.9$  Hz, 1 H, 6''-H), 7.76 (d,  $J=7.8$  Hz, 1 H, 4''-H), 7.66-7.73 (m, 2 H, 5', 5''-H), 7.04 (s, 1 H, 6-H). EI-HRMS  $m/z$  518.0583 ( $M^+$ ), calcd for  $C_{26}H_{12}F_6O_5$ : 518.0589.

#### 4.1.25.

##### *5-hydroxy-3,9-bis(4-(trifluoromethyl)phenyl)pyrano[2,3-f]chromene-4,10-dione (26a)*

White solid. Yield 39%. mp 202.6-203.5 °C;  $^1H$  NMR (500 MHz,  $DMSO-d_6$ )  $\delta$  13.67 (s, 1 H, OH), 8.93 (s, 1 H, 2-H), 8.55 (s, 1 H, 8-H), 7.84 (dd,  $J=8.5, 9.3$  Hz, 4 H, 3', 5', 3'', 5''-H), 7.78 (s, 4 H, 2', 6', 2'', 6''-H), 7.02 (s, 1 H, 6-H). EI-HRMS  $m/z$  518.0582 ( $M^+$ ), calcd for  $C_{26}H_{12}F_6O_5$ : 518.0589.

#### 4.1.26.

##### *5-hydroxy-3,9-bis(4-(trifluoromethoxy)phenyl)pyrano[2,3-f]chromene-4,10-dione (27a)*

Yellow solid. Yield 33%. mp 175.7-176.6 °C;  $^1H$  NMR (500 MHz,  $DMSO-d_6$ )  $\delta$  13.70 (s, 1 H, OH), 8.87 (s, 1 H, 2-H), 8.49 (s, 1 H, 8-H), 7.75 (d,  $J=8.8$  Hz, 2 H, 3', 5'-H), 7.67 (d,  $J=8.7$  Hz, 2 H, 3'', 5''-H), 7.46 (d,  $J=8.1$  Hz, 2 H, 2', 6'-H), 7.42 (d,  $J=8.1$  Hz, 2 H, 2'', 6''-H), 6.99 (s, 1 H, 6-H);  $^{13}C$  NMR (125 MHz,  $DMSO-d_6$ )  $\delta$  180.1, 172.3, 164.0, 161.2, 156.5, 155.9, 152.9, 148.4, 148.1, 131.0, 131.0, 130.6, 129.1, 124.0, 123.9, 123.9, 123.1, 121.3, 121.3, 119.8 (d,  $J=255.3$  Hz, 1 C), 119.7 (d,  $J=232.1$  Hz, 1 C), 116.2, 116.2, 108.9, 106.4, 99.6. EIMS  $m/z$  550.0 ( $M^+$ ).

#### 4.1.27. *5-hydroxy-3,9-di(thiophen-2-yl)pyrano[2,3-f]chromene-4,10-dione (28a)*

Yellow solid. Yield 40%. mp 222.2-222.9 °C;  $^1H$  NMR (500 MHz,  $DMSO-d_6$ )  $\delta$  13.49 (s, 1 H, OH), 9.33 (s, 1 H, 2-H), 8.93 (s, 1 H, 8-H), 7.74 (dd,  $J=1.0, 3.8$  Hz, 1 H, 3'-H), 7.70 (dd,  $J=0.9, 4.9$  Hz, 1 H, 3''-H), 7.62-7.63 (m, 2 H, 5', 5''-H), 7.19 (dd,  $J=3.8, 5.1$  Hz, 1 H, 4'-H), 7.13 (dd,  $J=4.1, 4.9$  Hz, 1 H, 4''-H), 7.03 (s, 1 H, 6-H);  $^{13}C$  NMR (125 MHz,  $DMSO-d_6$ )  $\delta$  178.7, 171.5, 163.7, 160.7, 155.6, 154.7, 151.0, 131.0, 129.7, 128.3, 127.9, 126.7, 126.2, 125.3, 124.2, 119.5, 118.9, 108.6, 105.9, 99.6. EIMS  $m/z$  394.0 ( $M^+$ ).

#### 4.1.28. *5-hydroxy-3,9-di(naphthalen-1-yl)pyrano[2,3-f]chromene-4,10-dione (29a)*

Orange solid. Yield 10%. mp 170.8-171.4 °C;  $^1H$  NMR (500 MHz,  $DMSO-d_6$ )  $\delta$  13.74 (s, 1 H, OH), 8.78 (s, 1 H, 2-H), 8.46 (s, 1 H, 8-H), 7.98-8.05 (m, 4 H, 5', 8', 5'', 8''-H), 7.80 (d,  $J=8.5$  Hz, 1 H, 4'-H), 7.72 (d,  $J=8.8$  Hz, 1 H, 4''-H), 7.47-7.62 (m, 8 H, 2', 3', 6', 7', 2'', 3'', 6'', 7''-H), 7.11 (s, 1 H, 6-H);  $^{13}C$  NMR (125 MHz,  $DMSO-d_6$ )  $\delta$  180.8, 173.0, 164.0, 161.7, 157.1, 156.4, 153.2, 133.0, 133.0, 132.0, 131.9, 129.7, 129.1, 128.7, 128.5, 128.2, 128.0, 128.0, 128.0, 126.3, 126.1, 126.1, 125.9, 125.8,

125.8, 125.4, 125.4, 125.4, 124.5, 109.0, 106.7, 99.6. EIMS  $m/z$  482.1 ( $M^+$ ).

4.1.29. *5-hydroxy-3,9-diphenylpyrano[2,3-f]chromene-4,10-dione (30a)*

White solid. Yield 51%. mp 210.9-211.5 °C;  $^1\text{H}$  NMR (500 MHz,  $\text{DMSO-}d_6$ )  $\delta$  13.84 (s, 1 H, OH), 8.83 (s, 1 H, 2-H), 8.43 (s, 1 H, 8-H), 7.64 (d,  $J = 7.0$  Hz, 2 H, 2', 6'-H), 7.71 (d,  $J = 7.0$  Hz, 2 H, 2'', 6''-H), 7.38-7.49 (m, 6 H, 3', 4', 5', 3'', 4'', 5''-H), 6.99 (s, 1 H, 6-H);  $^{13}\text{C}$  NMR (125 MHz,  $\text{DMSO-}d_6$ )  $\delta$  180.4, 172.6, 164.0, 161.2, 156.2, 156.2, 156.0, 152.4, 131.3, 129.9, 129.1, 129.1, 129.1, 128.5, 128.3, 128.3, 128.1, 128.1, 125.4, 124.3, 108.9, 106.6, 99.4, 99.4. EIMS  $m/z$  382.0 ( $M^+$ ).

4.1.30. *3,9-dicyclopropyl-5-hydroxypyrano[2,3-f]chromene-4,10-dione (31a)*

Brown solid. Yield 7%. mp 216.0-216.9 °C;  $^1\text{H}$  NMR (500 MHz,  $\text{DMSO-}d_6$ )  $\delta$  13.78 (s, 1 H, OH), 8.37 (s, 1 H, 2-H), 7.93 (s, 1 H, 8-H), 6.81 (s, 1 H, 6-H), 1.72-1.83 (m, 2 H, 1', 1''-H), 0.84-0.86 (m, 2 H, 2'-H), 0.74-0.80 (m, 4 H, 3', 2''-H), 0.59-0.62 (m, 2 H, 3''-H);  $^{13}\text{C}$  NMR (125 MHz,  $\text{DMSO-}d_6$ )  $\delta$  182.0, 174.3, 163.3, 161.2, 155.7, 154.1, 150.0, 126.6, 126.0, 107.7, 105.6, 98.9, 6.5, 5.9, 5.6, 5.6, 5.5, 5.5. EIMS  $m/z$  310.1 ( $M^+$ ).

4.1.31. *5-hydroxy-3,7-di-o-tolylpyrano[3,2-g]chromene-4,6-dione (4b)*

Pale-brown powder. Yield 46%. mp 278.3-279.0 °C;  $^1\text{H}$  NMR (500 MHz,  $\text{DMSO-}d_6$ )  $\delta$  14.65 (s, 1 H, OH), 8.36 (s, 2 H, 2, 8-H), 7.29-7.35 (m, 5 H, ArH), 7.22-7.27 (m, 4 H, ArH), 2.18 (s, 6 H,  $2\times\text{CH}_3$ );  $^{13}\text{C}$  NMR (125 MHz,  $\text{DMSO-}d_6$ )  $\delta$  177.5, 177.5, 164.2, 159.4, 159.4, 154.7, 154.7, 137.6, 137.6, 130.7, 130.7, 130.7, 130.7, 129.8, 129.8, 128.5, 128.5, 125.6, 125.6, 125.0, 125.0, 108.1, 108.1, 95.4, 19.6, 19.6. EIMS  $m/z$  410.2 ( $M^+$ ).

4.1.32. *5-hydroxy-3,7-di-m-tolylpyrano[3,2-g]chromene-4,6-dione (5b)*

Yellow solid. Yield 34%. mp 262.9-263.7 °C;  $^1\text{H}$  NMR (500 MHz,  $\text{DMSO-}d_6$ )  $\delta$  14.75 (s, 1 H, OH), 8.46 (s, 2 H, 2, 8-H), 7.31-7.36 (m, 6 H, ArH), 7.21-7.24 (m, 3 H, ArH), 2.35 (s, 6 H,  $2\times\text{CH}_3$ );  $^{13}\text{C}$  NMR (125 MHz,  $\text{DMSO-}d_6$ )  $\delta$  177.7, 177.7, 164.5, 159.1, 159.1, 154.2, 154.2, 137.3, 137.3, 130.6, 130.6, 129.6, 129.6, 128.8, 128.8, 128.1, 128.1, 126.1, 126.1, 124.0, 124.0, 108.2, 108.2, 95.2, 21.0, 21.0. EIMS  $m/z$  410.2 ( $M^+$ ).

4.1.33. *5-hydroxy-3,7-di-p-tolylpyrano[3,2-g]chromene-4,6-dione (6b)*

Yellow solid. Yield 48%. mp 330.5-331.4 °C;  $^1\text{H}$  NMR (500 MHz,  $\text{DMSO-}d_6$ )  $\delta$  14.79 (s, 1 H, OH), 8.46 (s, 2 H, 2, 8-H), 7.45 (d,  $J = 7.4$  Hz, 4 H, ArH), 7.26 (d,  $J = 7.4$  Hz, 5 H, ArH), 2.34 (s, 6 H,  $2\times\text{CH}_3$ ). EI-HRMS  $m/z$  410.1162 ( $M^+$ ), calcd for

$C_{26}H_{18}O_5$ : 410.1154.

4.1.34. 5-hydroxy-3,7-bis(2-methoxyphenyl)pyrano[3,2-g]chromene-4,6-dione (7b)

Brown powder. Yield 8%. mp >390 °C;  $^1H$  NMR (500 MHz, DMSO- $d_6$ )  $\delta$  7.79 (s, 2 H, 2, 8-H), 7.08-7.12 (m, 2 H, ArH), 6.67 (d,  $J$  = 6.2 Hz, 2 H, ArH), 6.58-6.60 (m, 4 H, ArH), 6.24 (s, 1 H, 10-H), 3.26 (s, 6 H, 2 $\times$ OCH $_3$ );  $^{13}C$  NMR (125 MHz, DMSO- $d_6$ )  $\delta$  177.8, 177.8, 173.1, 160.9, 160.9, 156.5, 156.5, 152.5, 152.5, 130.5, 130.5, 128.9, 128.9, 121.3, 121.3, 120.3, 120.3, 119.4, 119.4, 112.2, 112.2, 110.4, 110.4, 89.8, 54.8, 54.8. EIMS  $m/z$  442.1 ( $M^+$ ).

4.1.35. 5-hydroxy-3,7-bis(3-methoxyphenyl)pyrano[3,2-g]chromene-4,6-dione (8b)

Yellow solid. Yield 21%. mp 206.1-206.7 °C;  $^1H$  NMR (500 MHz, DMSO- $d_6$ )  $\delta$  14.76 (s, 1 H, OH), 8.51 (s, 2 H, 2, 8-H), 7.36 (t,  $J$  = 8.2 Hz, 2 H, 5', 5''-H), 7.26 (s, 1 H, 10-H), 7.13-7.14 (m, 4 H, ArH), 6.97-6.99 (m, 2 H, ArH), 3.79 (s, 6 H, 2 $\times$ OCH $_3$ );  $^{13}C$  NMR (125 MHz, DMSO- $d_6$ )  $\delta$  177.5, 177.5, 164.5, 159.0, 159.0, 159.0, 159.0, 154.4, 154.4, 131.9, 131.9, 129.2, 129.2, 123.7, 123.7, 121.3, 121.3, 114.7, 114.7, 113.7, 113.7, 108.2, 108.2, 95.2, 55.1, 55.1. EIMS  $m/z$  442.1 ( $M^+$ ).

4.1.36. 5-hydroxy-3,7-bis(4-methoxyphenyl)pyrano[3,2-g]chromene-4,6-dione (9b)

Brown solid. Yield 27%. mp 309.2-310.1 °C;  $^1H$  NMR (500 MHz, DMSO- $d_6$ )  $\delta$  14.81 (s, 1 H, OH), 8.44 (s, 2 H, 2, 8-H), 7.50 (d,  $J$  = 8.6 Hz, 4 H, ArH), 7.24 (s, 1 H, 10-H), 7.01 (d,  $J$  = 8.6 Hz, 4 H, ArH), 3.79 (s, 6 H, 2 $\times$ OCH $_3$ ). EI-HRMS  $m/z$  442.1045 ( $M^+$ ), calcd for  $C_{26}H_{18}O_7$ : 442.1053.

4.1.37. 5-hydroxy-3,7-bis(3-hydroxyphenyl)pyrano[3,2-g]chromene-4,6-dione (10b)

Dark-green solid. Yield 18%. mp 303.8-304.7 °C;  $^1H$  NMR (500 MHz, DMSO- $d_6$ )  $\delta$  14.80 (s, 1 H, OH), 9.50 (s, 2 H, 2 $\times$ OH), 8.45 (s, 2 H, 2, 8-H), 7.21-7.25 (m, 3 H, ArH), 6.99-6.99 (m, 2 H, ArH), 6.95 (d,  $J$  = 7.7 Hz, 2 H, ArH), 6.79-6.81 (m, 2 H, ArH);  $^{13}C$  NMR (125 MHz, DMSO- $d_6$ )  $\delta$  177.6, 177.6, 164.5, 159.1, 159.1, 157.1, 157.1, 154.2, 154.2, 131.8, 131.8, 129.2, 129.2, 123.9, 123.9, 119.6, 119.6, 116.1, 116.1, 115.2, 115.2, 108.2, 108.2, 95.2. EIMS  $m/z$  414.1 ( $M^+$ ).

4.1.38. 3,7-bis(3,4-dimethoxyphenyl)-5-hydroxypyrano[3,2-g]chromene-4,6-dione (11b)

Yellow needle crystal. Yield 53%. mp 282.4-283.1 °C;  $^1H$  NMR (500 MHz, DMSO- $d_6$ )  $\delta$  14.83 (s, 1 H, OH), 8.47 (s, 2 H, 2, 8-H), 7.24 (s, 1 H, 10-H), 7.17 (d,  $J$  = 1.9 Hz, 2 H, 2', 2''-H), 7.12 (dd,  $J$  = 1.9, 8.4 Hz, 2 H, 6', 6''-H), 7.02 (d,  $J$  = 8.4 Hz, 2 H, 5', 5''-H), 3.79 (s, 12 H, 4 $\times$ OCH $_3$ );  $^{13}C$  NMR (125 MHz, DMSO- $d_6$ )  $\delta$  177.8,

177.8, 164.5, 159.0, 159.0, 153.8, 153.8, 148.9, 148.9, 148.3, 148.3, 123.6, 123.6, 123.0, 123.0, 121.5, 121.5, 112.9, 112.9, 111.6, 111.6, 108.1, 108.1, 95.1, 55.6, 55.6, 55.5, 55.5. EIMS  $m/z$  502.2 ( $M^+$ ).

4.1.39. *5-hydroxy-3,7-bis(3,4,5-trimethoxyphenyl)pyrano[3,2-g]chromene-4,6-dione (12b)*

Brown powder. Yield 8%. mp 160.3-161.2 °C;  $^1\text{H}$  NMR (500 MHz,  $\text{DMSO-}d_6$ )  $\delta$  14.79 (s, 1 H, OH), 8.52 (s, 2 H, 2, 8-H), 7.28 (s, 1 H, 10-H), 6.89 (s, 4 H, 2', 6', 2'', 6''-H), 3.81 (s, 12 H, 4 $\times$ OCH<sub>3</sub>), 3.70 (s, 6 H, 2 $\times$ OCH<sub>3</sub>);  $^{13}\text{C}$  NMR (125 MHz,  $\text{DMSO-}d_6$ )  $\delta$  177.7, 177.7, 164.6, 159.0, 159.0, 154.4, 154.4, 152.6, 152.6, 152.6, 152.6, 137.6, 137.6, 126.1, 126.1, 123.8, 123.8, 108.1, 108.1, 106.7, 106.7, 106.7, 106.7, 95.3, 60.1, 60.1, 60.1, 60.1, 56.0, 56.0. EIMS  $m/z$  562.2 ( $M^+$ ).

4.1.40. *3,7-bis(2-fluorophenyl)-5-hydroxypyrano[3,2-g]chromene-4,6-dione (14b)*

Yellow solid. Yield 42%. mp 280.5-281.4 °C;  $^1\text{H}$  NMR (500 MHz,  $\text{DMSO-}d_6$ )  $\delta$  14.50 (s, 1 H, OH), 8.52 (s, 2 H, 2, 8-H), 7.45-7.52 (m, 4 H, ArH), 7.28-7.35 (m, 5 H, ArH);  $^{13}\text{C}$  NMR (125 MHz,  $\text{DMSO-}d_6$ )  $\delta$  176.7, 176.7, 164.0, 160.0 (d,  $J = 246.0$  Hz, 2 C), 159.3, 159.3, 155.4, 155.4, 132.2 (d,  $J = 2.3$  Hz, 2 C), 130.8 (d,  $J = 8.1$  Hz, 2 C), 124.3 (d,  $J = 21.5$  Hz, 2 C), 119.9, 119.9, 118.5 (d,  $J = 15.5$  Hz, 2 C), 115.5 (d,  $J = 21.5$  Hz, 2 C), 108.1, 108.1, 95.7. EIMS  $m/z$  418.1 ( $M^+$ ).

4.1.41. *3,7-bis(3-fluorophenyl)-5-hydroxypyrano[3,2-g]chromene-4,6-dione (15b)*

Green-yellow solid. Yield 48%. 287.7 °C sublimation;  $^1\text{H}$  NMR (500 MHz,  $\text{DMSO-}d_6$ )  $\delta$  14.69 (s, 1 H, OH), 8.60 (s, 2 H, 2, 8-H), 7.48-7.53 (m, 2 H, ArH), 7.43-7.46 (m, 4 H, ArH), 7.35 (s, 1 H, 10-H), 7.24-7.28 (m, 2 H, ArH). EI-HRMS  $m/z$  418.0659 ( $M^+$ ), calcd for  $\text{C}_{24}\text{H}_{12}\text{F}_2\text{O}_5$ : 418.0653.

4.1.42. *3,7-bis(4-fluorophenyl)-5-hydroxypyrano[3,2-g]chromene-4,6-dione (16b)*

Green-yellow solid. Yield 68%. 283.0 °C sublimation;  $^1\text{H}$  NMR (500 MHz,  $\text{DMSO-}d_6$ )  $\delta$  14.71 (s, 1 H, OH), 8.52 (s, 2 H, 2, 8-H), 7.60-7.63 (m, 4 H, ArH), 7.27-7.31 (m, 5 H, ArH). EI-HRMS  $m/z$  418.0653 ( $M^+$ ), calcd for  $\text{C}_{24}\text{H}_{12}\text{F}_2\text{O}_5$ : 418.0653.

4.1.43. *3,7-bis(2-chlorophenyl)-5-hydroxypyrano[3,2-g]chromene-4,6-dione (17b)*

Red powder. Yield 16%. mp 284.1-284.8 °C;  $^1\text{H}$  NMR (500 MHz,  $\text{DMSO-}d_6$ )  $\delta$  14.45 (s, 1 H, OH), 8.48 (s, 2 H, 2, 8-H), 7.58 (d,  $J = 7.7$  Hz, 2 H, ArH), 7.42-7.49 (m, 6 H, ArH), 7.36 (s, 1 H, 10-H);  $^{13}\text{C}$  NMR (125 MHz,  $\text{DMSO-}d_6$ )  $\delta$  176.7, 176.7, 164.0, 159.4, 159.4, 155.3, 155.3, 133.9, 133.9, 132.6, 132.6, 130.4, 130.4, 130.0, 130.0.

129.3, 129.3, 127.2, 127.2, 123.4, 123.4, 108.1, 108.1, 95.8. EIMS  $m/z$  415.0 (M-36).

4.1.44. *3,7-bis(3-chlorophenyl)-5-hydroxypyrano[3,2-g]chromene-4,6-dione (18b)*

Green-yellow solid. Yield 28%. mp 322.8-323.5 °C;  $^1\text{H}$  NMR (500 MHz, DMSO- $d_6$ )  $\delta$  14.55 (s, 1 H, OH), 8.52 (s, 2 H, 2, 8-H), 7.66-7.67 (m, 2 H, 2', 2''-H), 7.54-7.56 (m, 2 H, ArH), 7.45-7.50 (m, 4 H, ArH), 7.23 (s, 1 H, 10-H). EI-HRMS  $m/z$  450.0067 ( $\text{M}^+$ ), calcd for  $\text{C}_{24}\text{H}_{12}\text{Cl}_2\text{O}_5$ : 450.0062.

4.1.45. *3,7-bis(4-chlorophenyl)-5-hydroxypyrano[3,2-g]chromene-4,6-dione (19b)*

Green-yellow solid. Yield 27%. mp 328.8-329.7 °C;  $^1\text{H}$  NMR (500 MHz, DMSO- $d_6$ )  $\delta$  14.68 (s, 1 H, OH), 8.55 (s, 2 H, 2, 8-H), 7.61 (d,  $J = 8.2$  Hz, 4 H, ArH), 7.53 (d,  $J = 8.2$  Hz, 4 H, ArH), 7.31 (s, 1 H, 10-H). EI-HRMS  $m/z$  450.0068 ( $\text{M}^+$ ), calcd for  $\text{C}_{24}\text{H}_{12}\text{Cl}_2\text{O}_5$ : 450.0062.

4.1.46. *5-hydroxy-3,7-bis(2-nitrophenyl)pyrano[3,2-g]chromene-4,6-dione (20b)*

Brown solid. Yield 16%. mp 270.7-271.5 °C;  $^1\text{H}$  NMR (500 MHz, DMSO- $d_6$ )  $\delta$  14.14 (s, 1 H, OH), 8.69 (s, 2 H, 2, 8-H), 8.14-8.16 (m, 2 H, ArH), 7.85-7.88 (m, 2 H, ArH), 7.72-7.75 (m, 2 H, ArH), 7.62-7.63 (m, 2 H, ArH), 7.44 (s, 1 H, 10-H);  $^{13}\text{C}$  NMR (125 MHz, DMSO- $d_6$ )  $\delta$  176.4, 176.4, 164.0, 159.5, 159.5, 154.0, 154.0, 148.9, 148.9, 134.0, 134.0, 132.6, 132.6, 130.2, 130.2, 125.1, 125.1, 124.4, 124.4, 123.3, 123.3, 107.5, 107.5, 95.0. ESIMS  $m/z$  473.2 (M+1).

4.1.47. *3,7-bis(2-chloro-6-fluorophenyl)-5-hydroxypyrano[3,2-g]chromene-4,6-dione (22b)*

Brown solid. Yield 22%. mp 206.5-207.3 °C;  $^1\text{H}$  NMR (500 MHz, DMSO- $d_6$ )  $\delta$  14.24 (s, 1 H, OH), 8.64 (s, 2 H, 2, 8-H), 7.53-7.58 (m, 2 H, 5', 5''-H), 7.49 (d,  $J = 8.1$  Hz, 2 H, 3', 3''-H), 7.43 (s, 1 H, 10-H), 7.36-7.39 (m, 2 H, 4', 4''-H);  $^{13}\text{C}$  NMR (125 MHz, DMSO- $d_6$ )  $\delta$  176.2, 176.2, 163.8, 160.7 (d,  $J = 246.4$  Hz, 2 C), 159.5, 159.5, 156.7, 156.7, 135.1 (d,  $J = 3.0$  Hz, 2 C), 131.7 (d,  $J = 9.4$  Hz, 2 C), 125.4 (d,  $J = 2.6$  Hz, 2 C), 118.2 (d,  $J = 19.6$  Hz, 2 C), 117.2, 117.2, 114.5 (d,  $J = 22.4$  Hz, 2 C), 108.1, 108.1, 96.3. EIMS  $m/z$  451.0 ( $\text{M}^+$ ).

4.1.48.

*5-hydroxy-3,7-bis(2-(trifluoromethyl)phenyl)pyrano[3,2-g]chromene-4,6-dione (24b)*

Light-yellow solid. Yield 16%. mp 192.9-193.5 °C;  $^1\text{H}$  NMR (500 MHz, DMSO- $d_6$ )  $\delta$  14.34 (s, 1 H, OH), 8.45 (s, 2 H, 2, 8-H), 7.86 (d,  $J = 7.8$  Hz, 2 H, ArH), 7.75-7.78 (m, 2 H, ArH), 7.67-7.70 (m, 2 H, ArH), 7.52 (d,  $J = 7.5$  Hz, 2 H, ArH), 7.37 (s, 1 H, 10-H). EI-HRMS  $m/z$  518.0580 ( $\text{M}^+$ ), calcd for  $\text{C}_{26}\text{H}_{12}\text{F}_6\text{O}_5$ : 518.0589.

## 4.1.49.

*5-hydroxy-3,7-bis(3-(trifluoromethyl)phenyl)pyrano[3,2-g]chromene-4,6-dione (25b)*

Brown solid. Yield 6%. mp 220.0-221.3 °C; <sup>1</sup>H NMR (500 MHz, DMSO-*d*<sub>6</sub>) δ 14.60 (s, 1 H, OH), 8.65 (s, 2 H, 2, 8-H), 7.95 (s, 2 H, 2', 2''-H), 7.87 (d, *J* = 7.5 Hz, 2 H, ArH), 7.78 (d, *J* = 7.7 Hz, 2 H, ArH), 7.68-7.71 (m, 2 H, 5', 5''-H), 7.35 (s, 1 H, 10-H). EI-HRMS *m/z* 518.0580 (M<sup>+</sup>), calcd for C<sub>26</sub>H<sub>12</sub>F<sub>6</sub>O<sub>5</sub>: 518.0589.

## 4.1.50.

*5-hydroxy-3,7-bis(4-(trifluoromethoxy)phenyl)pyrano[3,2-g]chromene-4,6-dione (27b)*

Green-yellow solid. Yield 23%. mp 282.9-283.7 °C; <sup>1</sup>H NMR (500 MHz, DMSO-*d*<sub>6</sub>) δ 14.66 (s, 1 H, OH), 8.57 (s, 2 H, 2, 8-H), 7.70 (d, *J* = 8.5 Hz, 4 H, ArH), 7.46 (d, *J* = 8.5 Hz, 4 H, ArH), 7.33 (s, 1 H, 10-H). EI-HRMS *m/z* 550.0482 (M<sup>+</sup>), calcd for C<sub>26</sub>H<sub>12</sub>F<sub>6</sub>O<sub>7</sub>: 550.0487.

4.1.51. *5-hydroxy-3,7-di(thiophen-2-yl)pyrano[3,2-g]chromene-4,6-dione (28b)*

Brown solid. Yield 3%. mp 344.1-344.7 °C; <sup>1</sup>H NMR (500 MHz, DMSO-*d*<sub>6</sub>) δ 14.51 (s, 1 H, OH), 8.98 (s, 2 H, 2, 8-H), 7.63-7.66 (m, 4 H, 3', 5', 3'', 5''-H), 7.35 (s, 1 H, 10-H), 7.15 (dd, *J* = 3.8, 4.9 Hz, 2 H, 4', 4''-H); <sup>13</sup>C NMR (125 MHz, DMSO-*d*<sub>6</sub>) δ 176.3, 176.3, 164.2, 158.6, 158.6, 152.9, 152.9, 130.5, 130.5, 127.8, 127.8, 126.4, 126.4, 124.6, 124.6, 118.1, 118.1, 107.6, 107.6, 95.6. EIMS *m/z* 393.9 (M<sup>+</sup>).

4.1.52. *5-hydroxy-3,7-di(naphthalen-1-yl)pyrano[3,2-g]chromene-4,6-dione (29b)*

Orange solid. Yield 31%. mp 231.7-232.4 °C; <sup>1</sup>H NMR (500 MHz, DMSO-*d*<sub>6</sub>) δ 14.60 (s, 1 H, OH), 8.53 (s, 2 H, 2, 8-H), 7.99-8.03 (m, 4 H, ArH), 7.76 (d, *J* = 8.4 Hz, 2 H, ArH), 7.54-7.61 (m, 4 H, ArH), 7.48-7.52 (m, 4 H, ArH), 7.43 (s, 1 H, 10-H); <sup>13</sup>C NMR (125 MHz, DMSO-*d*<sub>6</sub>) δ 178.0, 178.0, 164.2, 159.6, 159.6, 155.1, 155.1, 133.0, 133.0, 132.0, 132.0, 128.9, 128.9, 128.9, 128.9, 128.4, 128.4, 128.1, 128.1, 126.2, 126.2, 126.0, 126.0, 125.8, 125.8, 125.4, 125.4, 124.1, 124.1, 108.2, 108.2, 95.5. EIMS *m/z* 482.1 (M<sup>+</sup>).

4.1.53. *5-hydroxy-3,7-diphenylpyrano[3,2-g]chromene-4,6-dione (30b)*

Yellow solid. Yield 33%. mp 298.2-299.1 °C; <sup>1</sup>H NMR (500 MHz, DMSO-*d*<sub>6</sub>) δ 14.77 (s, 1 H, OH), 8.51 (s, 2 H, 2, 8-H), 7.52 (d, *J* = 7.1 Hz, 4 H, 2', 6', 2'', 6''-H), 7.44-7.47 (m, 4 H, 3', 5', 3'', 5''-H), 7.39-7.42 (m, 2 H, 4', 4''-H), 7.29 (s, 1 H, 10-H); <sup>13</sup>C NMR (125 MHz, DMSO-*d*<sub>6</sub>) δ 177.6, 177.6, 164.5, 159.1, 159.1, 154.3, 154.3, 130.7, 130.7, 129.0, 129.0, 129.0, 129.0, 128.2, 128.2, 128.2, 128.2, 128.2, 128.2.

123.9, 123.9, 108.2, 108.2, 95.2. EIMS  $m/z$  382.1 ( $M^+$ ).

#### 4.1.54. 3,7-dicyclopropyl-5-hydroxypyran[3,2-g]chromene-4,6-dione (31b)

Brown solid. Yield 29%. mp 230.8-231.7 °C;  $^1\text{H}$  NMR (500 MHz,  $\text{DMSO-}d_6$ )  $\delta$  14.69 (s, 1 H, OH), 8.02 (s, 2 H, 2, 8-H), 7.04 (s, 1 H, 10-H), 1.71-1.76 (m, 2 H, ArH), 0.78-0.82 (m, 4 H, ArH), 0.61-0.64 (m, 4 H, ArH);  $^{13}\text{C}$  NMR (125 MHz,  $\text{DMSO-}d_6$ )  $\delta$  179.3, 179.3, 163.7, 159.0, 159.0, 152.0, 152.0, 125.0, 125.0, 107.1, 107.1, 94.8, 6.1, 6.1, 5.3, 5.3, 5.3, 5.3. EIMS  $m/z$  310.1 ( $M^+$ ).

### 4.2. Biological evaluation

#### 4.2.1. Cell line establishment

Flp-In<sup>TM</sup>-293 cells were cultured in DMEM medium supplemented with 10% fetal bovine serum and selected with 100  $\mu\text{g/mL}$  zeocin at 37 °C, 95% humidity and 5%  $\text{CO}_2$ . The *ABCBI*/pcDNA5 containing full length *ABCBI* cDNA was constructed in our previous studies [23, 24]. The constructed *ABCBI*/pcDNA5 plasmid and pOG44 (the Flprecombinase expression plasmid) were co-transfected into the Flp-In<sup>TM</sup>-293 cells and were selected on the basis of hygromycin B resistance. The protein and mRNA expressions of P-gp were confirmed by Western blot analysis and real-time quantitative RT-PCR, respectively, in our previous studies [23, 24]. Human cervical carcinoma cell line HeLaS3 was purchased from Bioresource Collection and Research Center (Hsinchu, Taiwan). The multidrug resistant human cervical cancer cell line KBvin was kindly provided by Dr. Kuo-Hsiung Lee (University of North Carolina, Chapel Hill, U.S.A) and maintained with vincristine in a fixed period.

#### 4.2.2. Calcein-AM uptake assay

For Calcein-AM uptake study,  $1 \times 10^5$  cells were placed on 96-well black plates and cultured overnight. After pre-incubation with warm Hanks' balanced salt solution (HBSS) for 30 min, test compounds were added for 30 min in triplicate. Then, Calcein AM (1  $\mu\text{M}$ ) was added and incubated for another 30 min. After washed by ice-cold HBSS, Calcein fluorescence generated within the cells was analyzed by the SpectraMax Gemini XS microplate spectrometer (Molecular Devices Co., Sunnyvale, CA, USA) with the excitation set at 485 nm and the emission set at 535 nm. Each experiment was performed at least three times, each in triplicate on different days.

#### 4.2.3. Cell viability assay

The effect of test compounds on the cell viability of Flp-In<sup>TM</sup>-293, *ABCBI*/Flp-In<sup>TM</sup>-293, HeLaS3, and KBvin cells was determined by SRB assay as previously described [25]. The influences of combinations of test compounds and

chemotherapeutic agents on cell proliferation were further evaluated by SRB assay as well.

### *4.3. Molecular modeling*

#### *4.3.1. Ligand preparation*

The structures of the benzodipyran derivatives **5a** and **5b** were built and energy minimized by Discovery studio 3.1. Full minimization tool was used to generate low energy 3D conformers of the minimized structures, default settings was used. The resultant ligand structures were eventually docked at drug binding domain of P-gp.

#### *4.3.2. Docking protocol*

To determine the probable binding site for compound **5a** and **5b**, the ligand structure was docked at drug binding domain of P-gp using the “LibDock” mode of Discovery Studio 3.1 with the default parameters. The protein crystal structure of mouse P-gp obtained from protein data bank (PDB ID: 4Q9I) [26].

## **Acknowledgments**

This work was supported by grants from the Ministry of Science and Technology of Taiwan (MOST104-2815-C-039-022-B; MOST103-2815-C-039-023-B; NSC101-2320-B-039-010-MY3) and China Medical University of Taiwan (CMU104-SR-22; CMU103-SR-23). The multidrug resistant human cervical cancer cell line KBvin was kindly provided by professor Kuo-Hsiung Lee (University of North Carolina, Chapel Hill, U.S.A.).

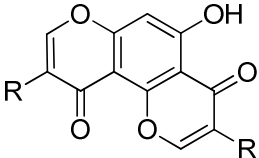
## **Appendix A. Supplementary data**

## References

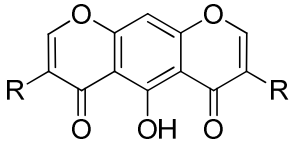
- [1] C. Ramalheite, J. Molnar, S. Mulhovo, V.E. Rosario, M.J. Ferreira, New potent P-glycoprotein modulators with the cucurbitane scaffold and their synergistic interaction with doxorubicin on resistant cancer cells, *Bioorg. Med. Chem.*, 17 (2009) 6942—6951.
- [2] L. Jiao, Q. Qiu, B. Liu, T. Zhao, W. Huang, H. Qian, Design, synthesis and evaluation of novel triazole core based P-glycoprotein-mediated multidrug resistance reversal agents, *Bioorg. Med. Chem.*, 22 (2014) 6857—6866.
- [3] G.A. Sawada, T.J. Raub, J. William Higgins, N.K. Brennan, T.M. Moore, G. Tomblin, M.R. Detty, Chalcogenopyrylium dyes as inhibitors/modulators of P-glycoprotein in multidrug-resistant cells, *Bioorg. Med. Chem.*, 16 (2008) 9745—9756.
- [4] S.V. Ambudkar, S. Dey, C.A. Hrycyna, M. Ramachandra, I. Pastan, M.M. Gottesman, Biochemical, cellular, and pharmacological aspects of the multidrug transporter, *Annu. Rev. Pharmacol. Toxicol.*, 39 (1999) 361—398.
- [5] D.W. Shen, S. Goldenberg, I. Pastan, M.M. Gottesman, Decreased accumulation of [<sup>14</sup>C]carboplatin in human cisplatin-resistant cells results from reduced energy-dependent uptake, *J. Cell Physiol.*, 183 (2000) 108—116.
- [6] C. Xu, C.Y. Li, A.N. Kong, Induction of phase I, II and III drug metabolism/transport by xenobiotics, *Arch. Pharm. Res.*, 28 (2005) 249—268.
- [7] S.W. Lowe, H.E. Ruley, T. Jacks, D.E. Housman, p53-dependent apoptosis modulates the cytotoxicity of anticancer agents, *Cell*, 74 (1993) 957—967.
- [8] E. Capparelli, L. Zinzi, M. Cantore, M. Contino, M.G. Perrone, G. Luurtsema, F. Berardi, R. Perrone, N.A. Colabufo, SAR studies on tetrahydroisoquinoline derivatives: the role of flexibility and bioisosterism to raise potency and selectivity toward P-glycoprotein, *J. Med. Chem.*, 57 (2014) 9983—9994.
- [9] Z. Wang, I.L. Wong, F.X. Li, C. Yang, Z. Liu, T. Jiang, T.F. Jiang, L.M. Chow, S.B. Wan, Optimization of permethyl ningalin B analogs as P-glycoprotein inhibitors, *Bioorg. Med. Chem.*, 23 (2015) 5566—5573.
- [10] T. Tsuruo, H. Iida, S. Tsukagoshi, Y. Sakurai, Overcoming of vincristine resistance in P388 leukemia in vivo and in vitro through enhanced cytotoxicity of vincristine and vinblastine by verapamil, *Cancer Res.*, 41 (1981) 1967—1972.
- [11] W. Van de Vrie, E.E. Gheuens, N.M. Durante, E.A. De Bruijn, R.L. Marquet, A.T. Van Oosterom, A.M. Eggermont, In vitro and in vivo chemosensitizing effect of cyclosporin A on an intrinsic multidrug-resistant rat colon tumour, *J. Cancer Res.*

- Clin. Oncol., 119 (1993) 609—614.
- [12] T. Tsuruo, H. Iida, Y. Kitatani, K. Yokota, S. Tsukagoshi, Y. Sakurai, Effects of quinidine and related compounds on cytotoxicity and cellular accumulation of vincristine and adriamycin in drug-resistant tumor cells, *Cancer Res.*, 44 (1984) 4303—4307.
- [13] V. Fischer, A. Rodriguez-Gascon, F. Heitz, R. Tynes, C. Hauck, D. Cohen, A.E. Vickers, The multidrug resistance modulator valspodar (PSC 833) is metabolized by human cytochrome P450 3A. Implications for drug-drug interactions and pharmacological activity of the main metabolite, *Drug Metab. Dispos.*, 26 (1998) 802—811.
- [14] E. Warner, D. Hedley, I. Andrulis, R. Myers, M. Trudeau, D. Warr, K.I. Pritchard, M. Blackstein, P.E. Goss, E. Franssen, K. Roche, S. Knight, S. Webster, R.A. Fraser, S. Oldfield, W. Hill, R. Kates, Phase II study of dexverapamil plus anthracycline in patients with metastatic breast cancer who have progressed on the same anthracycline regimen, *Clin. Cancer Res.*, 4 (1998) 1451—1457.
- [15] H. Thomas, H.M. Coley, Overcoming multidrug resistance in cancer: an update on the clinical strategy of inhibiting p-glycoprotein, *Cancer control : journal of the Moffitt Cancer Center*, 10 (2003) 159—165.
- [16] L. Pusztai, P. Wagner, N. Ibrahim, E. Rivera, R. Theriault, D. Booser, F.W. Symmans, F. Wong, G. Blumenschein, D.R. Fleming, R. Rouzier, G. Boniface, G.N. Hortobagyi, Phase II study of tariquidar, a selective P-glycoprotein inhibitor, in patients with chemotherapy-resistant, advanced breast carcinoma, *Cancer*, 104 (2005) 682—691.
- [17] J.S. Lagas, R.A. van Waterschoot, V.A. van Tilburg, M.J. Hillebrand, N. Lankheet, H. Rosing, J.H. Beijnen, A.H. Schinkel, Brain accumulation of dasatinib is restricted by P-glycoprotein (ABCB1) and breast cancer resistance protein (ABCG2) and can be enhanced by elacridar treatment, *Clin. Cancer Res.*, 15 (2009) 2344—2351.
- [18] I.E. Kuppens, E.O. Witteveen, R.C. Jewell, S.A. Radema, E.M. Paul, S.G. Mangum, J.H. Beijnen, E.E. Voest, J.H. Schellens, A phase I, randomized, open-label, parallel-cohort, dose-finding study of elacridar (GF120918) and oral topotecan in cancer patients, *Clin. Cancer Res.*, 13 (2007) 3276—3285.
- [19] C.A. McDevitt, R. Callaghan, How can we best use structural information on P-glycoprotein to design inhibitors?, *Pharmacol. Ther.*, 113 (2007) 429—441.
- [20] M.L. Amin, P-glycoprotein Inhibition for Optimal Drug Delivery, *Drug target insights*, 7 (2013) 27—34.
- [21] N.U.-D. Khan, N. Parveen, M.P. Singh, R. Singh, B. Achari, P.P.G. Dastidar, P.K. Dutta, Two isomeric benzodipyranone derivatives from *Calophyllum inophyllum*,

- Phytochemistry, 42 (1996) 1181—1183.
- [22] J.R. Bantick, H. Cairns, A. Chambers, R. Hazard, J. King, T.B. Lee, Benzodipyran derivatives with antiallergic activity, *J. Med. Chem.*, 19 (1976) 817—821.
- [23] C.C. Hung, M.H. Chiou, Y.N. Teng, Y.W. Hsieh, C.L. Huang, H.Y. Lane, Functional impact of ABCB1 variants on interactions between P-glycoprotein and methadone, *PLoS one*, 8 (2013) e59419.
- [24] C.C. Hung, H.H. Liou, YC-1, a novel potential anticancer agent, inhibit multidrug-resistant protein via cGMP-dependent pathway, *Invest. New Drugs*, 29 (2011) 1337—1346.
- [25] K. Nakagawa-Goto, A. Oda, E. Hamel, E. Ohkoshi, K.H. Lee, M. Goto, Development of a novel class of tubulin inhibitor from desmosdumotin B with a hydroxylated bicyclic B-ring, *J. Med. Chem.*, 58 (2015) 2378—2389.
- [26] P. Szewczyk, H. Tao, A.P. McGrath, M. Villaluz, S.D. Rees, S.C. Lee, R. Doshi, I.L. Urbatsch, Q. Zhang, G. Chang, Snapshots of ligand entry, malleable binding and induced helical movement in P-glycoprotein, *Acta Cryst. D*, 71 (2015) 732-741.

**Table 1.** Calcein-AM uptake assay of benzodipyrone derivatives.


CPD	R	P-gp inhibition fold	
		2.5 $\mu$ M	5 $\mu$ M
verapamil			2.39 $\pm$ 0.18
<b>4a</b>	2-methylphenyl	1.15 $\pm$ 0.04	1.53 $\pm$ 0.07
<b>5a</b>	3-methylphenyl	1.58 $\pm$ 0.06	2.05 $\pm$ 0.06
<b>6a</b>	4-methylphenyl	1.58 $\pm$ 0.07	2.04 $\pm$ 0.06
<b>7a</b>	2-methoxyphenyl	1.40 $\pm$ 0.09	1.56 $\pm$ 0.09
<b>8a</b>	3-methoxyphenyl	1.19 $\pm$ 0.05	1.28 $\pm$ 0.09
<b>9a</b>	4-methoxyphenyl	1.54 $\pm$ 0.04	1.84 $\pm$ 0.01
<b>10a</b>	3-hydroxyphenyl	1.01 $\pm$ 0.02	0.99 $\pm$ 0.02
<b>11a</b>	3,4-dimethoxyphenyl	1.45 $\pm$ 0.03	1.64 $\pm$ 0.03
<b>12a</b>	3,4,5-trimethoxyphenyl	0.76 $\pm$ 0.08	0.75 $\pm$ 0.05
<b>13a</b>	3,4-methylenedioxyphenyl	0.72 $\pm$ 0.08	0.70 $\pm$ 0.07
<b>14a</b>	2-fluorophenyl	0.76 $\pm$ 0.06	0.67 $\pm$ 0.05
<b>15a</b>	3-fluorophenyl	0.96 $\pm$ 0.03	0.82 $\pm$ 0.02
<b>16a</b>	4-fluorophenyl	0.92 $\pm$ 0.07	0.84 $\pm$ 0.08
<b>17a</b>	2-chlorophenyl	0.98 $\pm$ 0.05	1.09 $\pm$ 0.05
<b>18a</b>	3-chlorophenyl	0.83 $\pm$ 0.04	0.82 $\pm$ 0.03
<b>19a</b>	4-chlorophenyl	0.76 $\pm$ 0.03	0.82 $\pm$ 0.02
<b>20a</b>	2-nitrophenyl	0.98 $\pm$ 0.02	1.03 $\pm$ 0.01
<b>21a</b>	4-nitrophenyl	0.88 $\pm$ 0.02	0.75 $\pm$ 0.02
<b>22a</b>	2-chloro-6-fluorophenyl	0.66 $\pm$ 0.01	0.64 $\pm$ 0.03
<b>23a</b>	3,4-dichlorophenyl	0.80 $\pm$ 0.01	0.81 $\pm$ 0.01
<b>24a</b>	2-trifluoromethylphenyl	0.76 $\pm$ 0.01	0.81 $\pm$ 0.01
<b>25a</b>	3-trifluoromethylphenyl	1.10 $\pm$ 0.05	1.15 $\pm$ 0.04
<b>26a</b>	4-trifluoromethylphenyl	0.87 $\pm$ 0.01	0.90 $\pm$ 0.01
<b>27a</b>	4-trifluoromethoxyphenyl	0.97 $\pm$ 0.06	1.04 $\pm$ 0.08
<b>28a</b>	thiophen-2-yl	0.88 $\pm$ 0.04	0.83 $\pm$ 0.05
<b>29a</b>	1-naphthyl	0.87 $\pm$ 0.02	0.85 $\pm$ 0.02
<b>30a</b>	phenyl	1.04 $\pm$ 0.11	1.29 $\pm$ 0.04
<b>31a</b>	cyclopropyl	0.80 $\pm$ 0.06	0.63 $\pm$ 0.05

**Table 2.** Calcein-AM uptake assay of symmetrical benzodipyrone derivatives.


CPD	R	P-gp inhibition fold	
		2.5 $\mu$ M	5 $\mu$ M
verapamil			2.39 $\pm$ 0.18
<b>4b</b>	2-methylphenyl	0.87 $\pm$ 0.05	0.81 $\pm$ 0.02
<b>5b</b>	3-methylphenyl	0.86 $\pm$ 0.03	0.93 $\pm$ 0.05
<b>6b</b>	4-methylphenyl	1.62 $\pm$ 0.10	1.81 $\pm$ 0.12
<b>7b</b>	2-methoxyphenyl	0.76 $\pm$ 0.02	0.82 $\pm$ 0.05
<b>8b</b>	3-methoxyphenyl	1.00 $\pm$ 0.06	0.85 $\pm$ 0.04
<b>9b</b>	4-methoxyphenyl	0.87 $\pm$ 0.06	1.30 $\pm$ 0.02
<b>10b</b>	3-hydroxyphenyl	1.33 $\pm$ 0.06	1.19 $\pm$ 0.09
<b>11b</b>	3,4-dimethoxyphenyl	0.81 $\pm$ 0.01	0.86 $\pm$ 0.02
<b>12b</b>	3,4,5-trimethoxyphenyl	0.80 $\pm$ 0.03	0.72 $\pm$ 0.01
<b>14b</b>	2-fluorophenyl	0.92 $\pm$ 0.06	0.89 $\pm$ 0.05
<b>15b</b>	3-fluorophenyl	0.60 $\pm$ 0.03	0.75 $\pm$ 0.02
<b>16b</b>	4-fluorophenyl	0.85 $\pm$ 0.08	1.30 $\pm$ 0.01
<b>17b</b>	2-chlorophenyl	0.71 $\pm$ 0.01	0.85 $\pm$ 0.01
<b>18b</b>	3-chlorophenyl	0.50 $\pm$ 0.02	0.87 $\pm$ 0.09
<b>19b</b>	4-chlorophenyl	1.06 $\pm$ 0.05	1.08 $\pm$ 0.04
<b>20b</b>	2-nitrophenyl	0.85 $\pm$ 0.05	0.83 $\pm$ 0.02
<b>22b</b>	2-chloro-6-fluorophenyl	0.95 $\pm$ 0.02	1.06 $\pm$ 0.06
<b>24b</b>	2-trifluoromethylphenyl	1.32 $\pm$ 0.07	1.36 $\pm$ 0.07
<b>25b</b>	3-trifluoromethylphenyl	1.27 $\pm$ 0.08	1.18 $\pm$ 0.10
<b>27b</b>	4-trifluoromethoxyphenyl	0.62 $\pm$ 0.02	0.63 $\pm$ 0.12
<b>28b</b>	thiophen-2-yl	0.61 $\pm$ 0.04	0.67 $\pm$ 0.02
<b>29b</b>	1-naphthyl	0.72 $\pm$ 0.03	0.64 $\pm$ 0.02
<b>30b</b>	phenyl	1.04 $\pm$ 0.08	0.90 $\pm$ 0.05
<b>31b</b>	cyclopropyl	0.86 $\pm$ 0.02	0.86 $\pm$ 0.03

**Table 3.** Reversal effect of benzodipyranone derivatives on *ABCBI* substrates in Flp-In<sup>TM</sup>-293 and *ABCBI*/Flp-In<sup>TM</sup>-293 cell.<sup>a</sup>

	Flp-In <sup>TM</sup> -293		<i>ABCBI</i> /Flp-In <sup>TM</sup> -293	
	IC <sub>50</sub> (nM)	RF	IC <sub>50</sub> (nM)	RF
<b><u>Paclitaxel</u></b>	0.5387 ± 0.0610	1.0	644.78 ± 2.60	1.0
+5a (8 μM)	0.3664 ± 0.0045*	1.5	59.6 ± 0.72*	10.8
+5a (10 μM)	0.3065 ± 0.0149*	1.8	40.12 ± 1.37*	16.1
+9a (8 μM)	0.1992 ± 0.0656*	2.7	302.78 ± 44.35*	2.1
+9a (10 μM)	0.1278 ± 0.0173*	4.2	78.82 ± 5.04*	8.2
+11a (8 μM)	0.5352 ± 0.0066	1.0	73.14 ± 2.83*	8.8
+11a (10 μM)	0.4163 ± 0.0074	1.3	67.67 ± 3.12*	9.5
<b><u>Vincristine</u></b>	5.9705 ± 0.1791	1.0	823.13 ± 15.79	1.0
+5a (8 μM)	0.7608 ± 0.0231*	7.8	52.60 ± 0.93*	15.6
+5a (10 μM)	0.6595 ± 0.0117*	9.1	39.11 ± 1.07*	21.0
+9a (8 μM)	0.9091 ± 0.0064*	6.6	577.20 ± 11.88*	1.4
+9a (10 μM)	0.8448 ± 0.0075*	7.1	499.76 ± 19.66*	1.6
+11a (8 μM)	0.7623 ± 0.0012*	7.8	203.01 ± 29.35*	4.1
+11a (10 μM)	0.7324 ± 0.0062*	8.2	84.95 ± 8.72*	9.7
<b><u>Doxorubicin</u></b>	92.1164 ± 13.6856	1.0	914.83 ± 15.85	1.0
+5a (8 μM)	76.2722 ± 3.1190	1.2	664.36 ± 35.25*	1.4
+5a (10 μM)	58.0384 ± 1.8049*	1.6	586.26 ± 11.67*	1.6
+9a (8 μM)	97.5533 ± 3.0147	0.9	575.77 ± 14.99*	1.6
+9a (10 μM)	43.4454 ± 1.9503*	2.1	544.21 ± 9.30*	1.7
+11a (8 μM)	78.7184 ± 2.4492	1.2	597.21 ± 5.14*	1.5
+11a (10 μM)	71.0428 ± 1.7621	1.3	594.42 ± 5.91*	1.5

<sup>a</sup>RF : Reversal fold of benzodipyranone derivatives. RF = IC<sub>50</sub> of anticancer drugs to the cell / IC<sub>50</sub> of combination with benzodipyranone derivatives and anticancer drugs. \*p < 0.05 compared with substrate drug transport with tested compounds.

**Table 4.** Reversal effect of benzodipyranone derivatives on *ABCBI* substrates in HeLaS3 and KBvin cell.<sup>a</sup>

	HeLaS3		KBvin	
	IC <sub>50</sub> (nM)	RF	IC <sub>50</sub> (nM)	RF
<b><u>Paclitaxel</u></b>	4.2482 ± 0.0593	1.0	1196.09 ± 44.80	1.0
+5a (8 μM)	3.7307 ± 0.1888	1.1	62.86 ± 2.49*	19.0
+5a (10 μM)	3.0093 ± 0.3231	1.4	51.67 ± 0.26*	23.1
<b><u>Vincristine</u></b>	3.5543 ± 0.2879	1.0	2867.34 ± 142.36	1.0
+5a (8 μM)	0.7596 ± 0.0289*	4.7	389.77 ± 36.27*	7.4
+5a (10 μM)	0.4031 ± 0.0526*	8.8	96.49 ± 1.90*	29.7

<sup>a</sup>RF : Reversal fold of benzodipyranone derivatives. RF = IC<sub>50</sub> of anticancer drugs to the cell / IC<sub>50</sub> of combination with benzodipyranone derivatives and anticancer drugs. \*p < 0.05 compared with substrate drug transport with tested compounds.

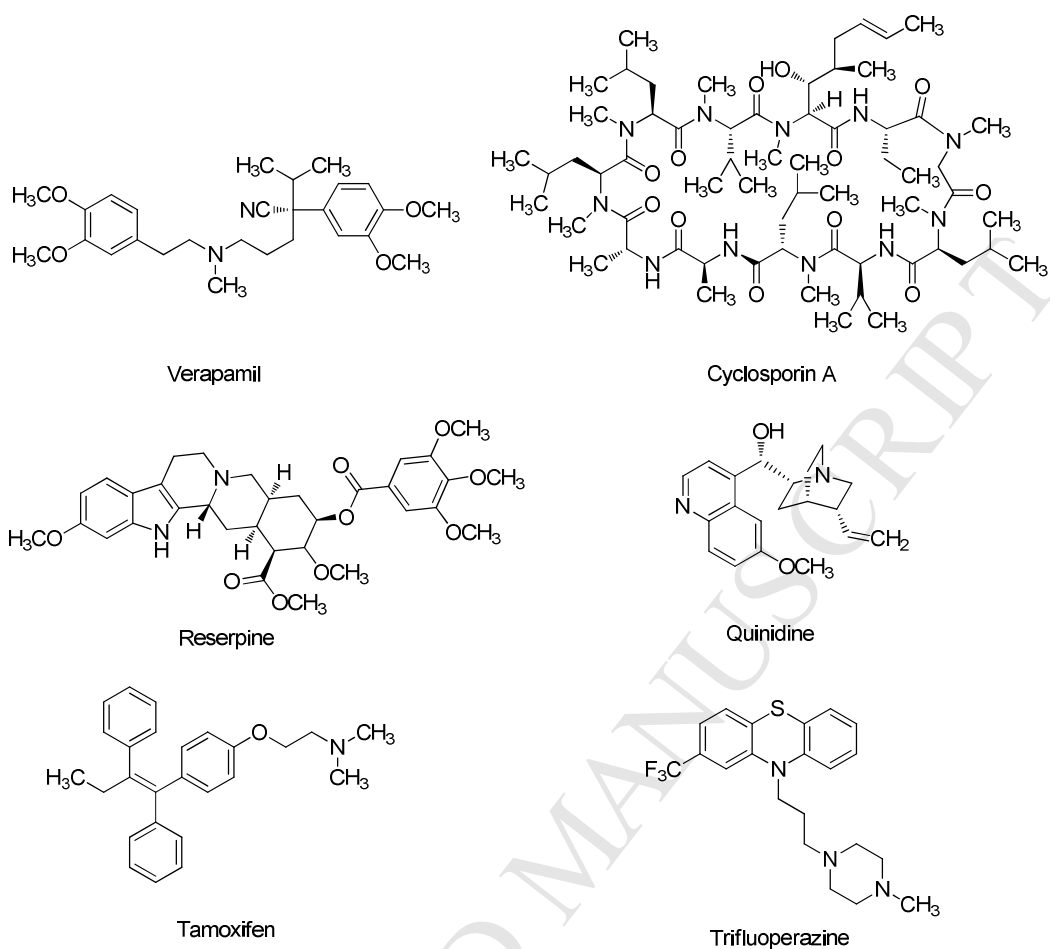
## Figure Legends

**Figure 1.** First-generation of P-gp inhibitors.

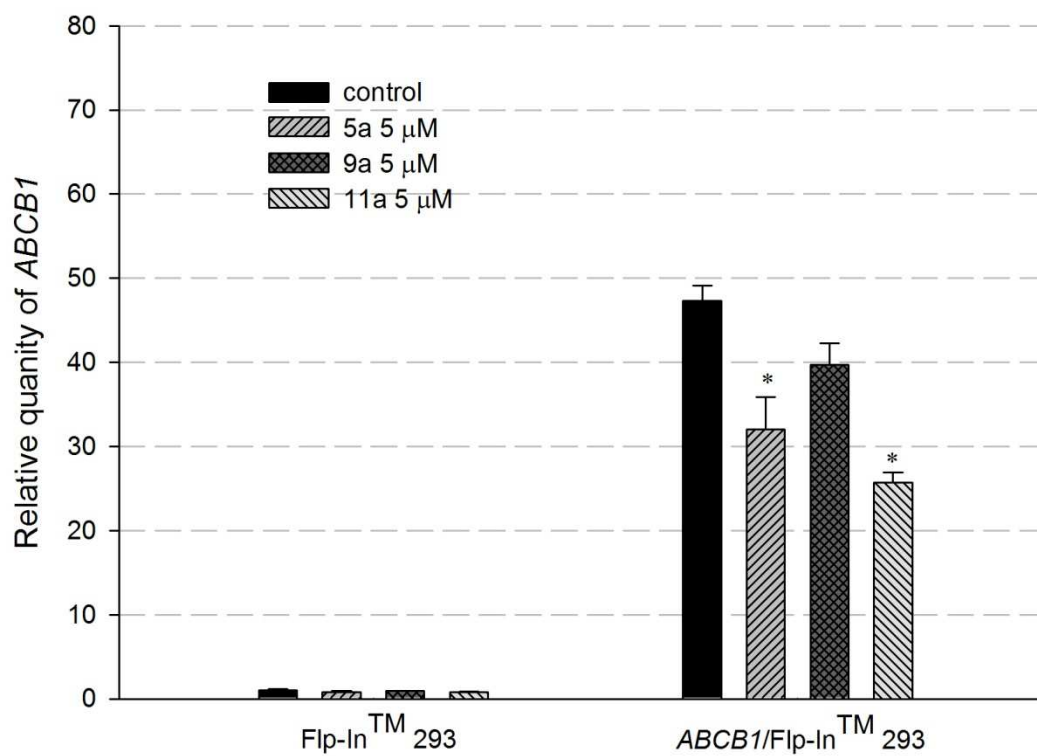
**Figure 2.** Second- and third-generation of P-gp inhibitors

**Figure 3.** *ABCB1* mRNA expression after treating the P-gp-transfected cell line *ABCB1/Flp-In<sup>TM</sup>-293* with benzodipyrone derivatives for 72 hr. Data were presented as mean  $\pm$  SE of three experiments, each in triplicate.

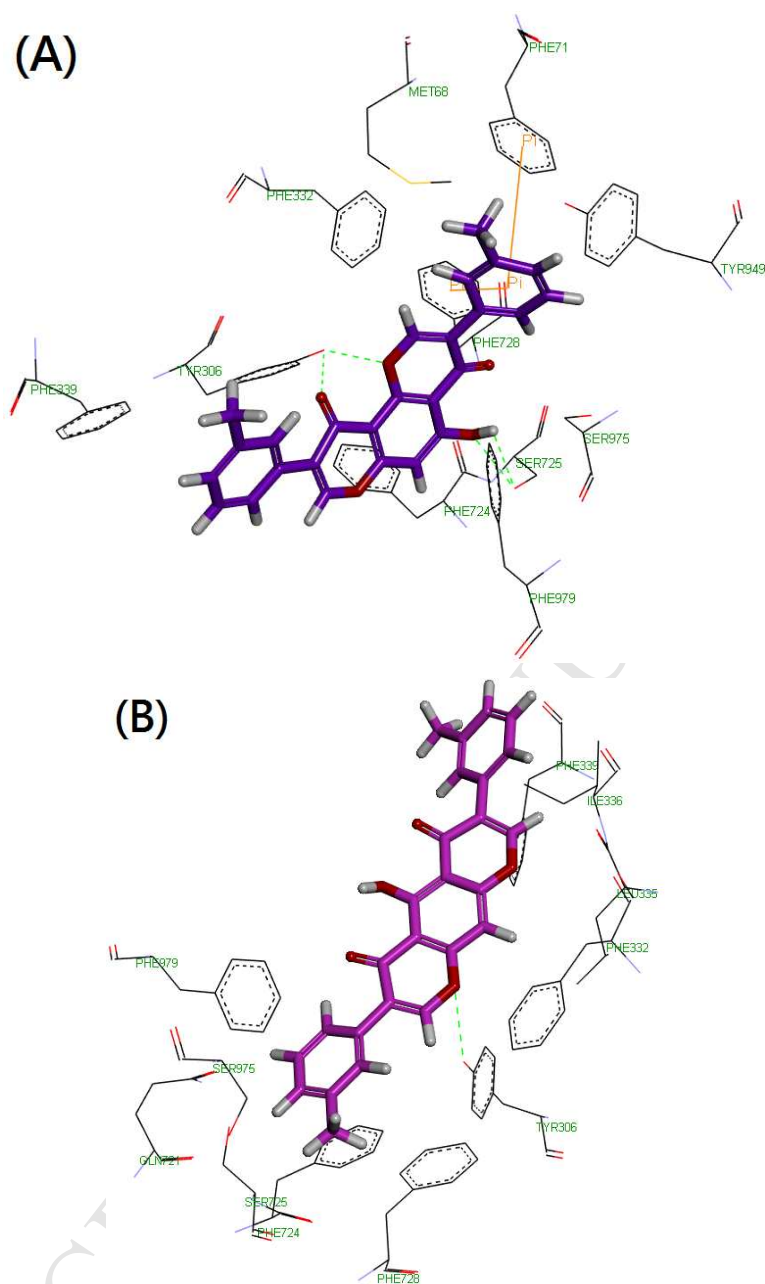
**Figure 4.** Docking interaction of compound **5a** and **5b** with P-gp. Selected amino acids are depicted as lines with the atoms colored as carbon, black; hydrogen, white; nitrogen, blue; oxygen, red; sulfur, yellow. Whereas the inhibitor is shown as a stick model with the same color scheme as above except carbon atoms are represented in purple (**5a**) and pink (**5b**). Hydrogen bonds are shown as light-green dashes. While  $\pi$ - $\pi$  stacking aromatic interactions are shown by orange lines.

**Figure 1.** First-generation of P-gp inhibitors



*ABCB1* gene expression

**Figure 3.** *ABCB1* mRNA expression after treating the P-gp-transfected cell line *ABCB1/Flp-In<sup>TM</sup>-293* with benzodipyrone derivatives for 72 hr. Data were presented as mean  $\pm$  SE of three experiments, each in triplicate.

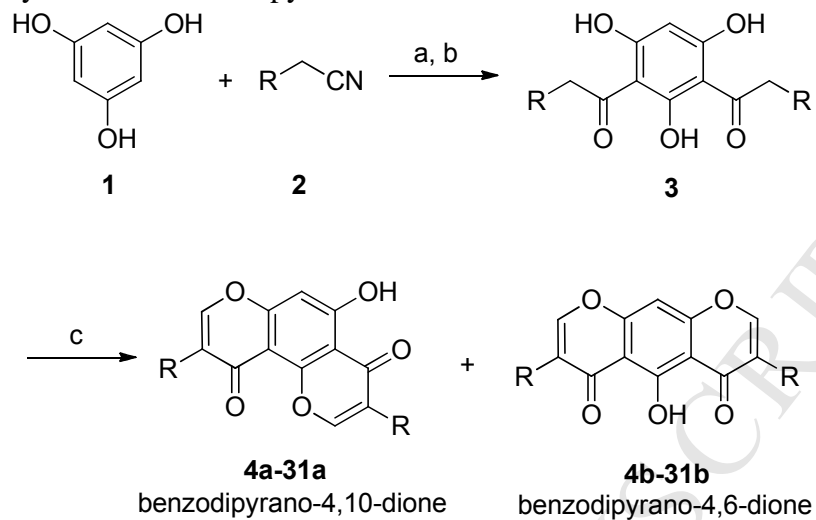


**Figure 4.** Docking interaction of compound **5a** and **5b** with P-gp. Selected amino acids are depicted as lines with the atoms colored as carbon, black; hydrogen, white; nitrogen, blue; oxygen, red; sulfur, yellow. Whereas the inhibitors is shown as a stick model with the same color scheme as above except carbon atoms are represented in purple (**5a**) and pink (**5b**). Hydrogen bonds are shown as light-green dashes. While  $\pi$ - $\pi$  stacking aromatic interactions are shown by orange lines.

**Scheme Legend**

**Scheme 1.** Synthesis of benzodipyrone derivatives.<sup>a</sup>

<sup>a</sup>Reagents and conditions: (a) HCl<sub>(g)</sub>, BF<sub>3</sub> · Et<sub>2</sub>O, rt.; (b) 1 M HCl, reflux.; (c) MsCl, DMF, BF<sub>3</sub> · Et<sub>2</sub>O, 120 °C.

**Scheme 1.** Synthesis of benzodipyrano derivatives.<sup>a</sup>

R = substituted aryl or cyclopropyl

<sup>a</sup>Reagents and conditions: (a)  $\text{HCl}_{(\text{g})}$ ,  $\text{BF}_3 \cdot \text{Et}_2\text{O}$ , rt.; (b) 1 M HCl, reflux.; (c) MsCl, DMF,  $\text{BF}_3 \cdot \text{Et}_2\text{O}$ , 120 °C.

- The novel 52 benzodipyrone analogs were synthesized and evaluated for their P-gp inhibitory activity in a P-gp transfected cell line, *ABCBI/Flp-In<sup>TM</sup>-293*.
- The compound **5a** can enable the increase of the intracellular accumulation of P-gp substrate Calcein-AM.
- The compound **5a** exhibited more potency on promoted anticancer drugs cytotoxicity by reversing P-gp-mediated drug resistance in both *ABCBI/Flp-In<sup>TM</sup>-293* and KBvin cell lines.
- The compound **5a** can enhance the sensitization of *ABCBI/Flp-In<sup>TM</sup>-293* and KBvin resistant cells line toward paclitaxel, vincristine, and doxorubicin.